# Rewakening of a Volcano: Activity Beneath Eyjafjallajökull Volcano from 1991 to 2009.

Type of paper: Research paper

Sigurlaug Hjaltadóttir (corresponding author)
slauga@vedur.is
Icelandic Meteorological Office, Bústaðavegi 9, 150 Reykjavík, Iceland
Nordic Volcanological Center, Institute of Earth Sciences, University of Iceland, Sturlugötu 9, 107 Reykjavík, Iceland

Kristín S. Vogfjörð
vogfjord@vedur.is
Icelandic Meteorological Office, Bústaðavegi 9, 150 Reykjavík, Iceland

Sigrún Hreinsdóttir
s.hreinsdottir@gns.cri.nz
Institute of Earth Sciences, Sturlugötu 9, 107 Reykjavík, Iceland
GNS Science, PO Box 30368, Lower Hutt 5040, New Zealand

Ragnar Slunga
ragnar.slunga@quakelook.se
QuakeLook Stockholm AB, Stockholm, Sweden

# Abstract

The ice-capped Eyjafjallajökull volcano, south Iceland, had been dormant for 170 years when the first signs of rewakening of the volcano were captured by seismic and geodetic measurements in 1994. These were the first clear observed unrest signs followed by 16 years of intermittent magmatic unrest culminating in 2010 when two eruptions broke out on the flank and at the summit. We analyze seismic data from 1991 through 2008 and GPS data from 1992 to May 2009 to infer magma movements beneath the volcano. The relocated earthquakes reveal an overall pipe-like pattern northeast of the summit crater, sporadically mapping the pathway of magma from the base of the crust towards an intrusion in the upper crust. During the study period three major seismic swarms were recorded. Two of them, in 1994 and 1999-2000, occurred in the upper and intermediate crust and accompanied crustal deformation centered at the southeastern flank. No uplift was detected during the 19-25 km deep 1996-swarm, near to the crust-mantle boundary, but the horizontal, ~E-W oriented T-axes indicate a period of tension/opening, suggesting magma intruding up into the base of the crust. The GPS measured deformation during 1999-2000 can be modelled as intrusion of a horizontal, circular sill with volume of 0.030 ± 0.007 $km^3$ at 5.0 ± 1.3 km depth. The less constrained 4.5-5 km deep sill-model for the 1994 episode indicates a three times smaller intruded volume (0.011 $km^3$) than during 1999-2000. In the years between/following the intrusions, contraction was observed at the southeastern flank. The contraction from 2001 to 2009.3 can be fitted by a circular sill model with a volume contraction of -0.0015 ± 0.0003 $km^3$/year at 5.5 ± 2.0 km depth. The accumulated volume change (~ -0.014 $km^3$) is much larger than expected due to solidification and cooling of magma alone and might partly be explained by degassing ($CO_2$) and mass loading effects within the crust due to the intruded magma.




**Keywords:** VT-earthquakes, double-difference relocations, intrusion, uplift, subsidence, sill model.

# 1. Introduction

Eyjafjallajökull volcano in south Iceland rises 1666 m a.s.l. and is partly covered by an ice cap (Figure 1a). The volcano has a prominent ridge shape, elongated in the east-west

direction, with an east-west-striking fissure swarm as well as a radial dyke system extending from the small summit crater (Jónsson, 1988). Geodetic measurements suggest negligible spreading rates (Geirsson et al., 2012) across the region and it lacks the prominent NE-SW rifting structures characteristic for the Eastern Volcanic Zone (EVZ) (Sæmundsson, 1979). The slopes of Eyjafjallajökull volcano have been eroded by the outlet-glaciers and rivers extending from the ice cap. Reversely magnitized rocks are found in the gullies on the south side of the volcano, indicating that volcanic activity has persisted for over 0.7 M years. In some places intrusion rock accounts for roughly 70% of the rock volume (Jónsson, 1985).

Eyjafjallajökull volcano is seismically relatively quiet, with low levels of activity between its intrusion/eruption phases. The neighbouring Katla volcano, overlain by the larger Mýrdalsjökull ice cap, shows more persistent seismic activity, especially at its western flank (Soosalu et al., 2006; Jónsdóttir et al., 2007; Jakobsdóttir, 2008). During the operation of the analog, single component, Icelandic Seismograph Network (ISN) between 1967 and 1990, only fourteen events were located at Eyjafjallajökull whilst hundreds of events were detected in Katla (IMO database ; Skjálftabréf, 1979; Einarsson and Brandsdóttir, 2000).



The number of detected earthquakes at Eyjafjallajökull volcano has risen substantially since the beginning of digital, automatic detection of seismicity by the SIL (South Iceland Lowland) network in 1991. Three main periods of unrest were recorded in Eyjafjallajökull prior to 2009; in 1994, 1996, and 1999-2000. The 1994 and 1999-2000 seismic swarms were accompanied by uplift, suggesting the formation of horizontal sill intrusions at 4.5-6.3 km depth below the volcano's southern flank (Pedersen and Sigmundsson, 2004 and 2006; Hooper et al., 2009, Sturkell et al., 2010). In 2009-2010 the volcano experienced an unrest period culminating in two very different eruptions, in March and April 2010 (Sigmundsson et al., 2010). Eyjafjallajökull volcano has only two to three known historic (last 1100 years) eruptions prior to 2010; a flank eruption around 920 (Óskarsson, 2009), a possible summit eruption in 1612 or 1613 (Jónson, 1774; Larsen, 1999) and summit eruption 1821-23 (Thoroddsen, 1925). In comparison twenty-one confirmed eruptions have been recorded for Katla volcano during the same period (Larsen, 2000).

In this paper we describe the seismic activity within Eyjafjallajökull recorded by the SIL network from 1991 through 2008, with emphasis on seismic swarms in 1994, 1996, and 1999-2000 and the associated deformation. The earthquakes are relocated using a double-difference

algorithm and focal mechanisms are analyzed. Available GPS geodetic data from the region are used to evalute and model the deformation during both periods of high seismic activity and the relative quiet periods.

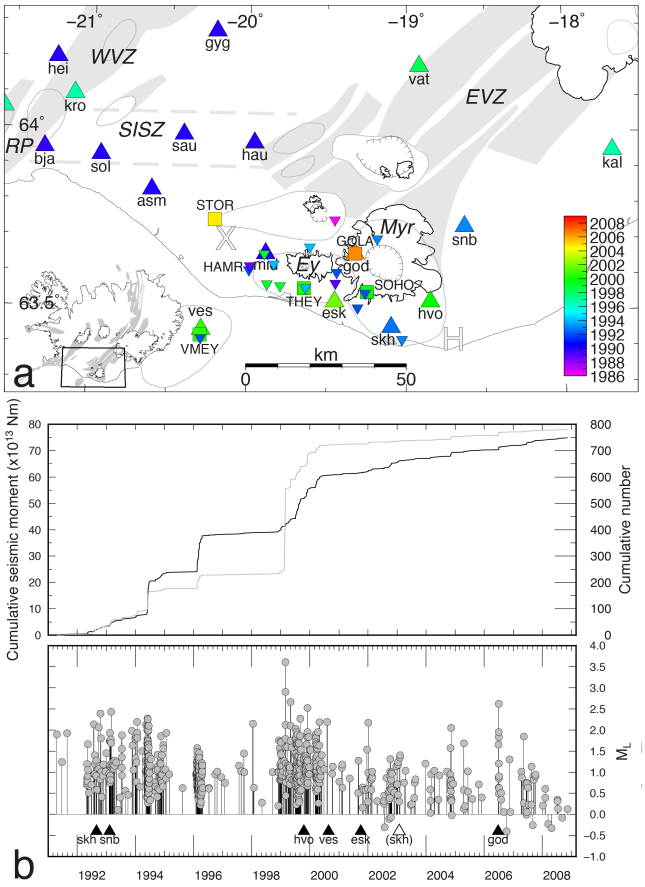




**Figure 1.** a) Map of South-Iceland and Eyjafjallajökull (Ey), with location of seismic- and GPS-stations, used in this study, coloured according to begin-date of automatic recording or installation date of benchmark (Table S1). Triangles denote seismic stations, squares CGPS stations and inverted triangles GPS campaign sites. Names of seismic stations and CGPS stations are shown. GPS-site HAMR was operating continuously from 2006 to 2008. Fissure swarms (grey areas), volcanic systems, and calderas are shown (from Sæmundsson and Einarsson, 1987) and main tectonic features: Reykjanes Peninsula (RP), the Western Volcanic Zone (WVZ), the Eastern Volcanic Zone (EVZ), and the South Icelandic Seismic Zone (SISZ) which takes up the transform motion between the RP and the EVZ. The caldera of the neighbouring Katla volcano is outlined, underlying the Mýrdalsjökull ice cap (Myr). Crustal thickness of the velocity model used in this research is based on an observed Moho reflection from the location marked by the X. The H marks the location of the deep earthquake swarm in December 2007 (Figure S6). b) Seismicity and earthquake magnitudes during the period 1991-2009. (Upper panel) Cumulative number of earthquakes (black line), cumulative seismic moment (grey), and (Lower panel) magnitude distribution of the 748 events used for analysis (shown in Figure 2b). Black triangles mark installation date of SIL-stations, open triangles mark the end of operation.

*(One or 1.5 column width)*

# 2. Seismic and geodetic data

## *2.1 Seismic data and analysis*

In 1989 and 1990 the first eight digital seismometers of the South Iceland Lowland (SIL) seismic network were installed. The network consists mostly of short period, three-component seismic stations (Stefánsson et al, 1993; Böðvarsson et al., 1996). In May 1991 the automatic detection system for the SIL network at the Icelandic Meteorological Office (IMO) became operational (Böðvarsson et al., 1996, 1999; Jakobsdóttir, 1998). The network sensitivity has increased over time with the installation of new seismic stations. In 1991-1992 only one station (**mid**) was located within 100 km distance from Eyjafjallajökull volcano, with events down to $M_l$~0.5 being detected. In August 1992 the SIL-station **skh** was added to the network 32 km south-east of Eyjafjallajökull and in February 1993 station **snb** was installed about 45 km to the ENE (Figure 1), improving the detection threshold down to $M_l$~0.3 and increasing the location accuracy of the system in the vicinity of Eyjafjallajökull (Figure 1). By the end of 2008 the network consisted of 55 seismic stations located around the plate boundary in Iceland, with 16 stations within ~100 km of Eyjafjallajökull, giving a completeness threshold of around $M_l$ 0.9 and event magnitudes down to $M_l$ -0.4 being detected (Figure 1).



The original seismic catalogue locations were acquired using the 1-D SIL-velocity model (Stefánsson et al., 1993) (Figure 2), which is based on velocity profiles in western/southwestern Iceland (Bjarnason et al, 1993). The SIL model has a $V_P/V_S$= 1.78 and no Moho-velocity discontinuity. The reading accuracy of P-wave arrivals can go down to the order of 0.1-0.2 s, which corresponds to approximately 600-1200 m in absolute location error. Applying cross-correlations techniques on the waveforms at each station, the relative travel time difference between similar and neighbouring earthquakes can be found with subsample accuracy at each station. This can decrease the relative location error between the events down to tens of metres (e.g. Slunga et al., 1995; Waldhauser and Ellsworth, 2000). We used the multi-event, double-difference relocation method of Slunga et al. (1995) to improve locations for our data set. For the relocations we tested two velocity models, the SIL-model and model P23 (blue line in Figure 2). P23 is based on the average of one-dimensional P- and S-wave velocity structures derived from two seismic profiles (P2 and P3) that extend eastwards from the Hengill triple junction and pass south of and north of the volcano (Vogfjörd et al., 2002). The $V_P/V_S$ ratio is 1.77 for the uppermost kilometres but changes to

1.78 at ~14 km depth. It has a Moho-boundary at a depth of 22 km, based on a Moho reflection at Fljótshlíð (X in Figure 1a), 28 km northwest of Eyjafjallajökull's summit, recorded at station **skh**. When using the SIL model, events from the 1994 swarm (1st relocation period) separated spatially from the 1999-2000 cluster (2nd period), both in depth and latitude. The difference was negligible when using the P23-model and further analysis was based on that model.

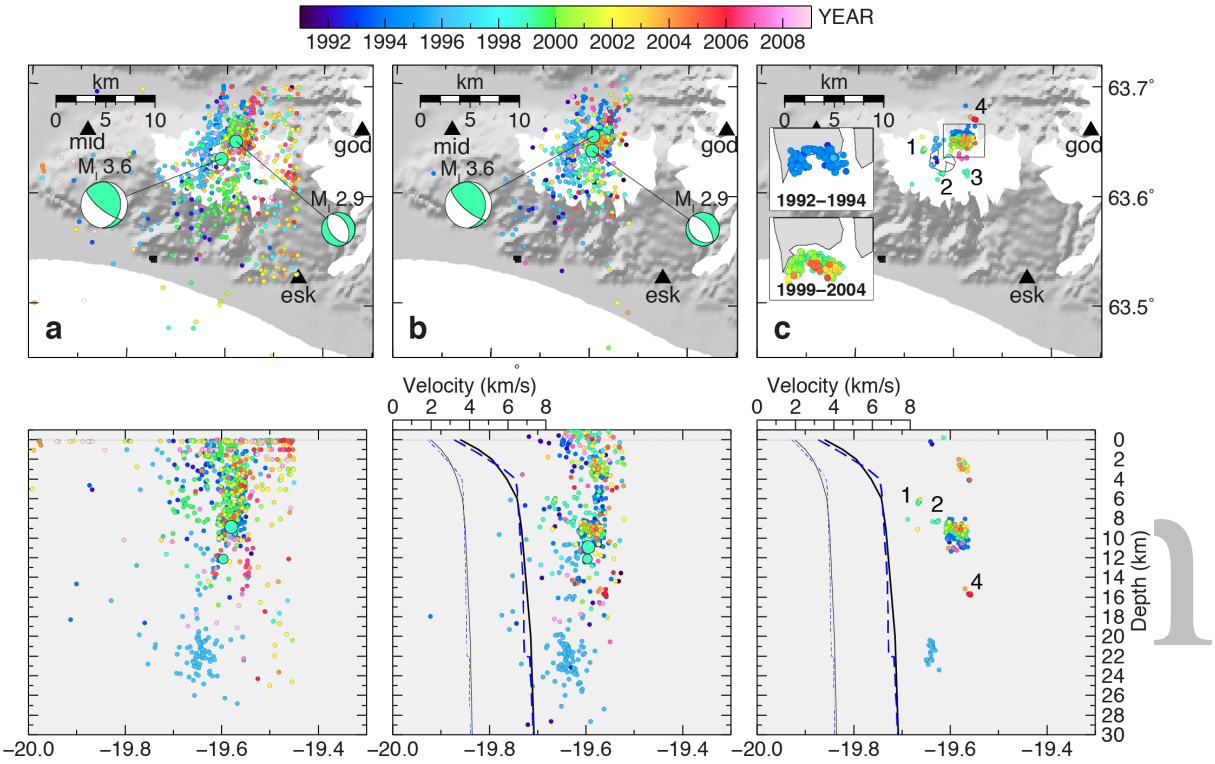


**Figure 2.** a: Original selection of catalogue events in map view (above) and vertical cross section viewed from south (below). Fault plane solutions (FPS) are shown for the two largest events of the data set, occurring on 1 March 1999. b: Relocated seismicity. The SIL-velocity model used for the original locations (black) and P23-velocity model (dashed blue) for the relocations are also shown for both P- and S-waves. FPS for the two largest events have been re-evaluated based on new locations. c: Selected relocated events with low relative error (within 100 m in latitude and longitude and 300 m in depth). The insets show handpicked selection of events (from events in b) that define the horseshoe shaped clusters during the two intrusion episodes.
(width: 2 columns or one page landscape)

Initially, all manually checked events from the SIL-catalogue between -20.0°E and -19.45°E and from 63.4°N to 63.7°N from 1991 through February 2009 were selected, a total of 922 events (Figure 2a). Since accurate clock information were not available or easily accessible for all stations until in June 1997, the data set was split into two separate time periods, before and after 14 June 1997. During the relocation, outliers and poorly correlating events are

eliminated from the catalogue. In addition, we did not consider shallow, scattered activity east of -19.52°E which is probably not related to Eyjafjallajökull volcano but occurs at Goðabunga, west of the Katla caldera rim (Einarsson and Brandsdóttir, 2000; Soosalu et al., 2006; Jónsdóttir et al., 2007; Jakobsdóttir, 2008), leaving 748 events (Figure 2b).

The improved earthquake locations were used to evaluate fault plane solutions using the method of Rögnvaldsson and Slunga (1993 and 1994). This method uses a grid search and comparison of calculated and measured amplitudes and manually picked polarities to create a range of possible double-couple solutions. We analysed the optimum solution, i.e. the one with the smallest measured vs. calculated amplitude fit error.

## *2.2. GPS measurements and analysis*

GPS geodetic measurements around Eyjafjallajökull have been conducted multiple times since 1989 to monitor the volcano. In 1999 a continuous GPS station (SOHO) was installed southeast of the volcano in response to increased activity and in 2000 the continuous GPS station THEY was installed at the southern flank of Eyjafjallajökull volcano, 550 m west of existing benchmark SELJ. In addition the GPS station HAMR was operated continuously from 2006 to 2008. Here we present a systematic re-analysis of all GPS data available from the Eyjafjallajökull geodetic network from August 1992 to May 2009.



The GPS data were analyzed using the GAMIT/GLOBK version 10.4 using from 25 (in 1992) to over 100 global CGPS stations in the analysis to evaluate site positions in the ITRF08 reference frame. In the analysis we solved for station coordinates, satellite orbit and Earth rotation parameters, estimating atmospheric zenith daily every two hours and using three atmospheric gradients per day. We used the IGS08 azimuth and elevation-dependent absolute phase center model with an elevation cutoff angle of 10° for the ground based antennas and applied the FES2004 ocean loading model. We used tsview of GGMATLAB (Herring, 2003) to evaluate more realistic uncertainties for continuous and semi continuous GPS stations, assuming a first order Gauss-Markov process.

The data were projected into an ITRF08 Eurasian fixed reference frame (Altamimi et al., 2012) and corrected for GIA model predictions for a layered earth model based on ice history of the four major glaciers in Iceland since 1890 (Árnadóttir et al., 2009; Schmidt et al., 2013, Peter Schmidt personal communication 2014). Árnadóttir et al. (2009) used vertical

deformation rates estimated from the ÍSNET nationwide GPS campaigns in 1993 and 2004 to evaluate the optimal earth parameters for their GIA model. The 1-D Earth model that best fitted the GPS data had an elastic thickness of 40 km and a viscosity of $10^{19}$ Pa s. Subtracting the horizontal deformation rates predicted by an optimal plate boundary model from the ISNET data, Árnadottir et al. (2009) observed a systematic signal of residual velocities directed away from the glaciers. A comparison to the horizontal velocities predicted by their preferred GIA model showed a close resemblance in the direction although in some places the predicted magnitudes were significantly smaller than the observed residuals most notably around Mýrdalsjökull and Eyjafjallajökull glaciers. Therefore, we investigated the effect of scaling the horizontal GIA-correction during our model calculations. We used $\chi^2_\nu$ minimization to find GIA scaling and optimum model parameters, $\chi^2_\upsilon = \sum_{j=1}^{3}\sum_{i=1}^{N}(\frac{u_{obs,i,j}-u_{model,i,j}}{\sigma_{i,j}})^2/(3N-\upsilon)$ where N denotes the number of stations and 3N is the total number of observations (velocities) (three components from N stations) and ν denotes the degree of freedom or free model parameters. We found a significant improvement in $\chi^2_\nu$ when using scaling factors between 1.2 and 1.8, with 1.6 giving the preferred model fit. Two $M_w$ 6.5 earthquakes occurred in South Iceland in June 2000. Coseismic offsets at the continuous sites THEY and SOHO are in agreement with model predictions by Pedersen et al. (2003) for these earthquakes. We used their coseismic model to correct all time series (Figure 3).



The GPS data were modeled assuming deformation in an elastic halfspace due to the formation and contraction of simple sill intrusions under the volcano (Fialko et al., 2001), using a grid search and the dMODELS software of Battaglia et al. (2013), modified to account for (different) elevation of GPS stations, to find the preferred solutions. We used a Poisson's ratio of 0.25.

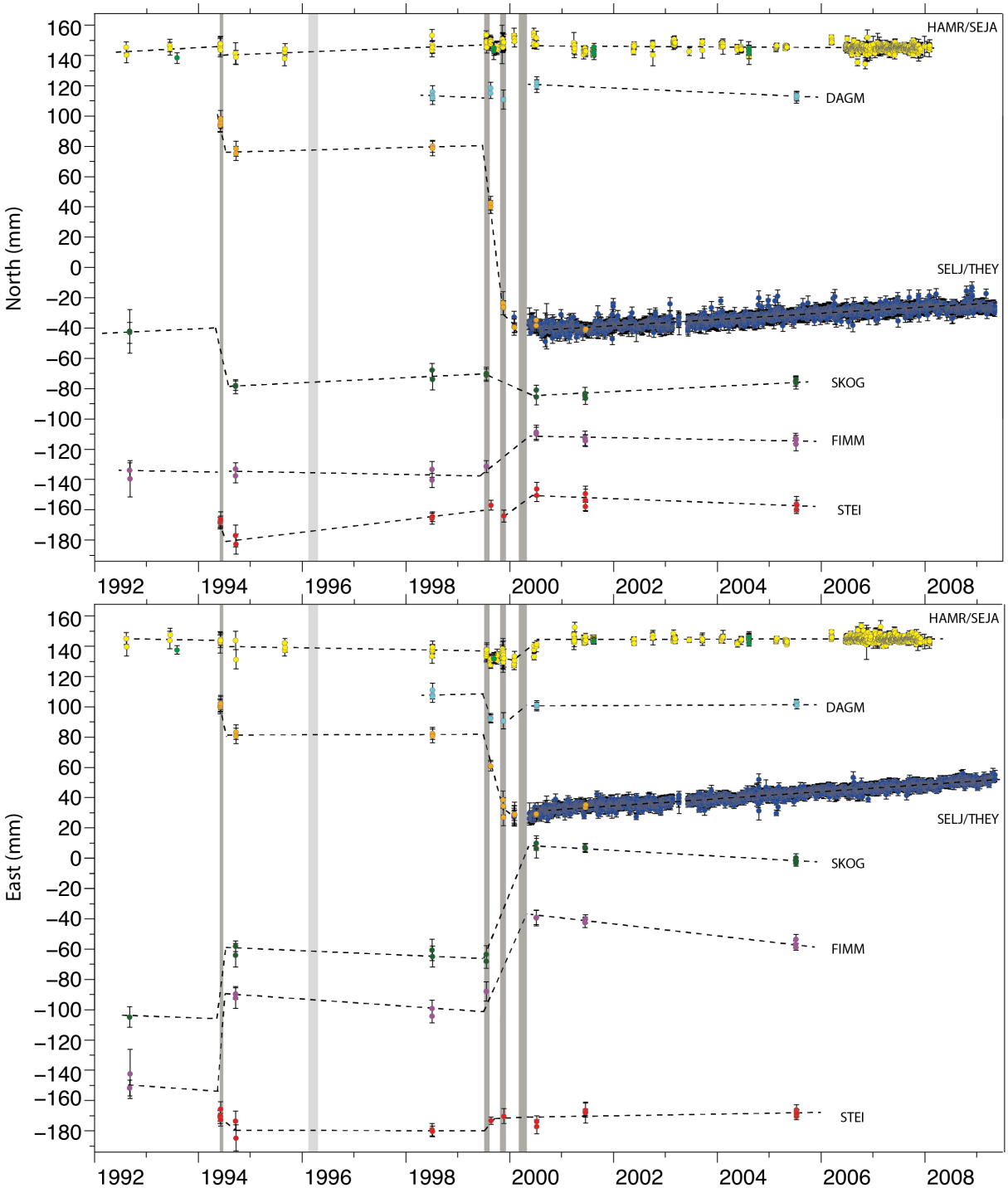


**Figure 3.** Time series for N- and E-components from selected GPS-stations around Eyjafjallajökull from 1992 to May 2009. The data are in Eurasian fixed ITRF08 reference frame, corrected for GIA from Schmidt et al., (2013) (scaling horizontal correction by 1.6) and coseismic offset due to the June 2000 SISZ earthquakes from Pedersen et al., (2003). Grey lines show periods of seismic swarm activity.

(Figure width: two columns)

## 3. Results

Our relocated catalogue for Eyjafjallajökull volcano, recorded by the SIL network from 1991 to 2008 consists of 748 events, ~64% of which occurred during the two intrusion events (in 1994 and 1999-2000) and the deep 1996 swarm. The earthquakes range from 0.5 km to 37 km depth with 95% of the events occuring above 23 km. Majority of the earthquakes form two clusters, an upper cluster at 2-5 km depth and a lower cluster at 8-11 km depth, below the northern flank of the volcano. A selection of well located earthquakes, with relative error less than 100 m in horizontal location and under 300 m in depth (Figure 2), indicate a horseshoe-shaped lower cluster, facing SSE and deepening eastwards (insert in Figure 2c). The deepest events, observed between 20 and 25 km depth, form a N-S-elongated cluster 2-3 km west of the main activity (light blue in Figure 2), with the best located events clustered below the ice cap, near the summit caldera. Additionally four small clusters with small relative error were observed within 2-3 km distance from the horseshoe-shaped cluster (numbered 1-4 in Figure 2).



The absolute location of the main cluster at 8-11 km is considerably deeper than the 6-8 km depth determined by Dahm and Brandsdóttir (1997) using four additional seismic stations temporarily deployed at Eyjafjallajökull during the 1994 swarm. It is thus likely that we have overestimated the depth of earthquakes in this main cluster. Additionally, data recorded after the installation of the station **god** (Figure 1), east of Eyjafjallajökull in 2006, suggest that the main cluster is located approximately 2 km farther south than indicated by pre 2006 data, or just east of the summit crater (Hjaltadóttir, et al., 2009; Tarasewicz, 2011). The relative location accuracy of the events within the cluster is, however, good and its shape is well constrained and consistent with the E-W orientation and the eastwards deepening also observed by Dahm and Brandsdóttir (1997) during 1994.

The b-value from the magnitude-frequency relation (Gutenberg and Richter, 1944) was estimated both manually and by using the maximum likelihood (or curvature) method (Aki, 1965; Wyss et al., 1997, Wiemer, 2001). For the complete dataset a b-value between 1.4-1.6 was estimated (table 1), reflecting the b-value at shallow (0-5 km) and intermediate depths (7-13 km) where majority of the earthquakes took place. In the lower crust, at 13-17 km, the b-value decreases to 1.1, but increases again to a much higher b-value of 2.5-3 in the deepest

cluster, below 17 km depth. The sparse data in the 5-7 km interval do not fit well to the Gutenberg-Richter relation and give unreliable estimates.

| ***Depth [km]*** | ***#events*** | ***b manual*** | ***b max.curv.*** | Mc |
|---|---|---|---|---|
| all relocated events | 748 | 1.6 | 1.4 | 1.6 |
| 1.5-5 | 120 | 1.8 | 1.4 | 1.5 |
| 5-7 | 36 | (1.9) | (2.5) | (1.8) |
| 7-13 | 334 | 1.4 | 1.5 | 1.8 |
| 13-17 | 42 | 1.1 | 1.1 | 1.4 |
| 17-26 | 99 | 3.1 | 2.5 | 1.6 |

**Table 1.** The b-values and magnitude of completeness for Eyjafjallajökull volcano estimated for the whole dataset and five distinct depth intervals, using both manual fitting and the maximum curvature method.

The optimum focal mechanisms showed a wide range of fault plane solutions. A larger variation was found in the azimuth of the P-axes of the optimum fault plane solutions (FPS) but the T-axes showed a trend towards W and NE-SW. The majority of T-axes had small dips, between 5-15°, but 30-40° dips were also observed (Figure 4). In general, greater scattering of FPS was observed for events occurring in 1994 than in 1999, as is expected due to poorer station geometry.



The GPS data show inflation of the SE flank of the volcano both in 1994 and 1999, consistent with the formation of sill intrusions at around 5 km depth below the volcano (Figure 3, Figure 5). The 1999-2000 intrusion is better constrained by the GPS data with a best fitting model of $\chi_\nu^2 = 3.13$ giving a depth of 5.0 ± 1.3 km and a volume of 0.030 ± 0.007 km$^3$, in a agreement with the results of Pederson and Sigmundsson (2006) using InSAR data. The GPS data are not good enough to constrain the depth of the 1994 intrusion but assuming that the depth in 1994 was 5 km, as in 1999 and consistant with the estimates of Pedersen and Sigmundsson (2004), we get a considerably smaller volume of 0.011 km$^3$ with $\chi_\nu^2$ of 14.

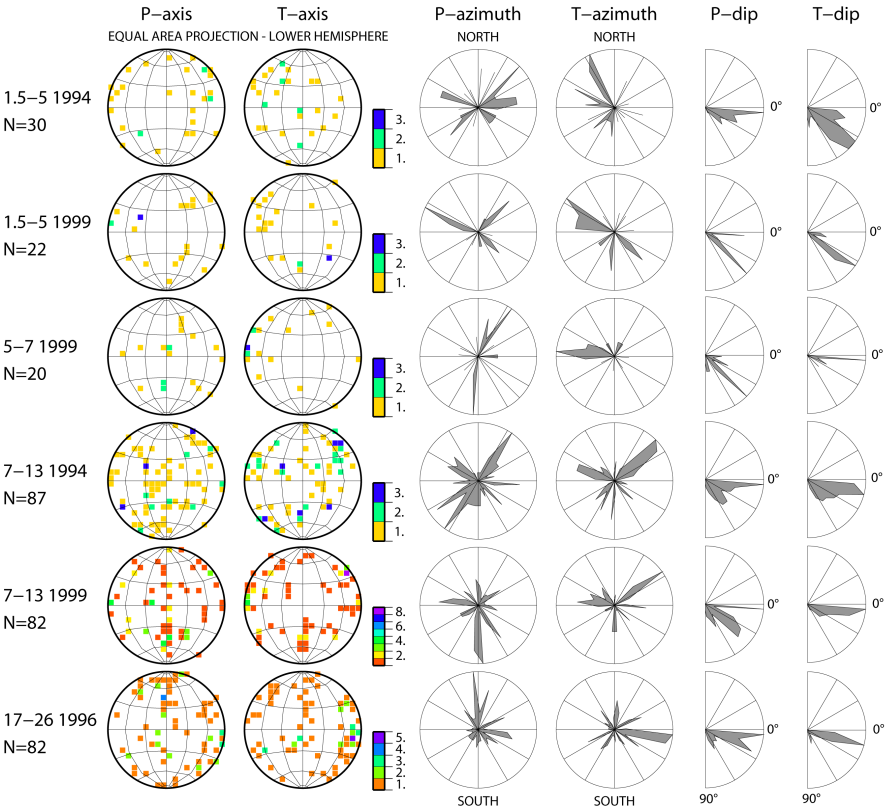


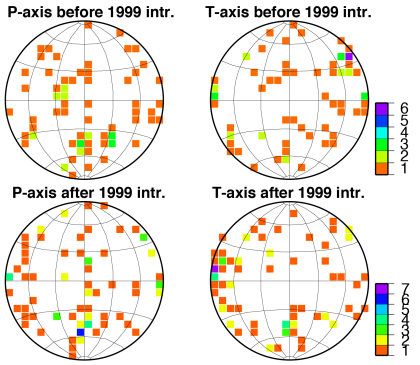




**Figure 4.** Upper: Mechanisms in selected depth intervals for the three main swarms. Number in first column, before year of swarm, indicates depth interval in kilometres. Colour scale shows number (density) of axes in each square on the plot. Lower: Distribution of P- and T-axis (on lower hemisphere) for events located between 7 and 13 km depth which occurred before the latter intrusion event (12 July 1996-July 1999) and after the main uplift had taken place (November 1999-August 2006).

In the time period between the two intrusions, 1994.7 – 1999.8, we see contraction of the southeast flank of the volcano, suggesting volume decrease of the intruded magma body (~1.3-3 mm/year horizontally at sites SELJ, FIMM, and SKOG, Figure 5). Contraction is also observed between 1 July 2000 and 30 April 2009, with twice the horizontal deformation rate

(3-5 mm/year). We modeled the data covering the 2nd contraction period assuming a volume change in a sill, using stations MORK, HAMR, MOLN, THEY, STEI, SKOG and FIMM. We applied GIA correction to the data and adjusted uncertainties of continuous stations by assuming that the noise is a first order Gauss Markov process. The results suggest a volume change of -1.5 ± 0.3 $\times 10^{-3}$ $km^3$/year in a sill at 5.5 ± 2.0 km depth with the best fitting/preferred model giving $\chi_\nu^2$=1.3.

| ***Year*** | ***Lat*** | ***Long*** | ***Depth (km)*** | ***Volume ($km^3$)*** | Radius (km) |
|---|---|---|---|---|---|
| 1994 | 63.596325 | -19.52930/ -19.52725 | 4.5/5.0 (fixed) | 0.011 | 1.550 |
| 1999 | 63.59655 | -19.58756 | 5.0 ± 1.3 | 0.030 ± 0.007 | 1.550 |
| 2000-2008 | 63.60733 | -19.57779 | 5.5±2.0 | -0.0015±0.0003* | 0.920 |

**Table 2.** Model parametres for the two intrusion events and the 2000.5-2009.3 contraction period. Volume change marked with * is estimated per year.

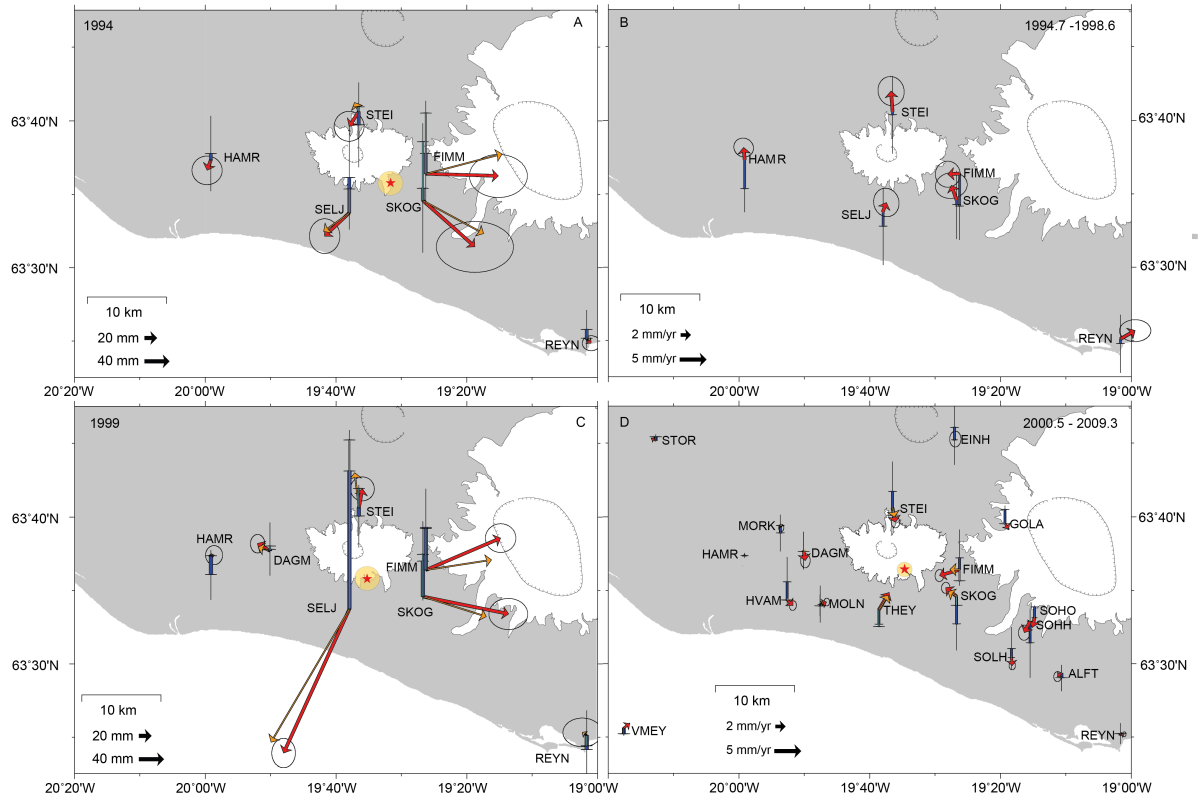


**Figure 5.** A and C: Estimated offset due to intrusions in 1994 and 1999-2000 (red for horizontal, blue for vertical) and the predicted model displacement (yellow for horizontal, turquise for vertical). B and D: Measured and GIA-corrected velocities and for the contraction periods (September 1994 – July 1998 and July 2000 – April 2009). Model velocities are also shown in panel D. Same colour scheme as in A and C.
(Figure width: 2 colmns)

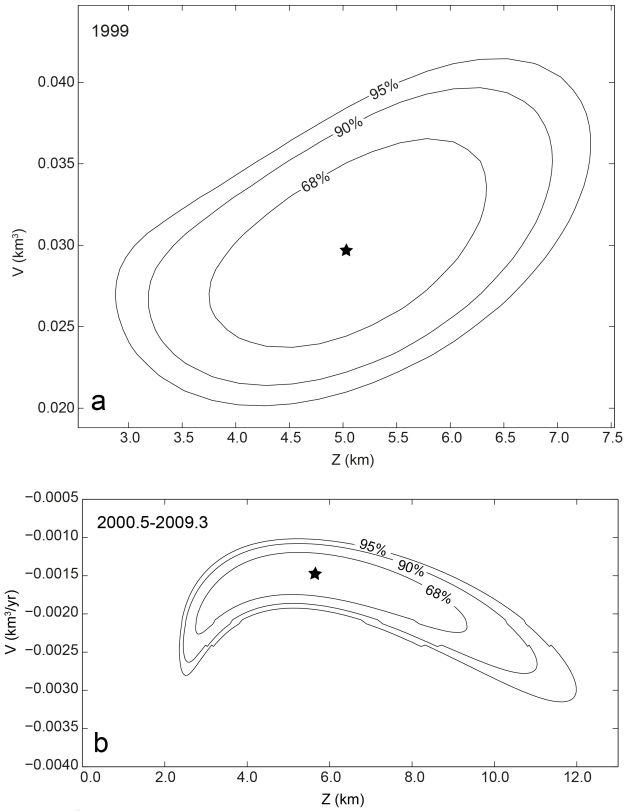


**Figure 6.** Fit of sill models with varying volume (that is varying ΔP/G where ΔP is pressure change, G the shear modulus and $\Delta V \propto \Delta P/G$) and depth. The star shows the parameters for best fitting model (lowest $\chi_\nu^2$) for the a) 1999-2000 intrusion and the b) 2000-2009 deflation period.
(Figure width: one column)



# 4. Temporal and spatial evolution

According to our seismic catalogue, Eyjafjallajökull volcano was relatively quiet up to 1992. Only three earthquakes were detected in 1991. Between May 1992 and April 1994 an average rate of three events per month was observed, with a maximum monthly rate of 8 and 11 events detected in May 1992 and February 1993, respectively. The earthquakes were located beneath the volcano's ice cap, both at shallow depths and between 6 and 11 km. In April and May 1992 a few deep earthquakes (16-29 km deep) were observed but their locations were uncertain due to the lack of near-field stations and poor azimuthal coverage. In 1993 the activity started to concentrate beneath the northern edge of the ice cap, at 8 to 11 km depth, but a few earthquakes were detected between 2 and 5 km depth (Figure S1).

On 29 May 1994 an earthquake swarm began beneath Eyjafjallajökull volcano associated with magma intruding into the volcano at around 5 km depth. Nearly 130 earthquakes were located with magnitudes ranging from $M_l$ 0.3–2.3. The earthquakes occurred mainly in two clusters beneath the northern flank, at 3–5 and 8–11 km depth, above and below the inferred sill intrusion (Figure 2; Sturkell et al., 2003, Pedersen and Sigmundsson, 2004). In the shallow cluster nearly half of the FPS indicate a thrust/strike-slip faulting (47% of T-axes oriented around NW, dipping 0-60° in Figure 3). After 22 June the activity dropped down to 5 events/month on average and from February 1995 to February 1996 only two earthquakes were detected.

Between 10 February and 22 April 1996 another swarm occurred beneath the central and northern part of the ice cap. About 140 earthquakes of magnitudes ranging from $M_l$ 0.2 to 1.6 were recorded. The swarm began with scattered activity, mostly recorded in the lower part of the crust (9-16 km), but then clustered at 19-25 km depth, near the base of the crust (Figure S2). This was the first such deep swarm recorded in Iceland by the SIL-network. FPS show predominantly normal motion, some also with a strike-slip component (with 68% of the the T-axis dipping close to horizontal and oriented close to east, 33% of P-axis striking near to N-S with small dip and 30% with more vertical P-axes, Figure 4). No significant deformation was observed associated with this swarm (Figure 3, Hooper, 2009). Following the swarm the activity dropped down to one event detected every 2-3 months on average until November 1998.



In December 1998 the seismicity rate increased again and on 1 March 1999 the two largest events in our dataset occurred, an $M_l$ 3.6, at 11 km depth with optimum fault plane solution indicating dominant reverse faulting and an $M_l$ 2.9 at 12 km depth with normal faulting. The seismicity rate stayed at a raised level until May 2000, with three main swarms; 4 July-12 September 1999, 20 October–3 December 1999, and 11 March–30 April 2000. As in 1994, the majority of the earthquakes ocurred in two clusters beneath the northern flank, with the lower cluster forming a horse-shoe shaped pattern (inset in Figure 2). A change was observed in August and September, when the seismicity partially migrated southward beneath the summit at 6-9 km depth (Figures S2 and S3). One small cluster of events (nr 3 in Figure 2) with low relative error is observed in July at 10 km depth south of the horseshoe-shaped cluster and two more (nr 1 and 2) southwest of it during the inflation phase, located at similar and slightly greater depths than the suggested sill. The activity gradually decreased after May

2000. GPS measurements conducted from July 1998 to July 2000 show inflation of the southeast flank of the volcano, with up to 130 mm SSW displacement and 110 mm uplift at a site south of the summit (Figure 5). According to the GPS time series the majority of the deformation took place prior to February 2000 (SELJ Figure 3) with a sill forming at 5 km depth. This is in a general agreement with InSAR observations (Pedersen and Sigmundsson, 2004; Hooper et al., 2009).

During the 1999-2000 swarm 45% of the FPSs examined at 1.5-5 km depth had T-axis oriented W to NW and accompanying P-axes indicating either predominantly strike-slip motion (27%) (nearly horizontal, NE-striking P-axes) or normal faulting (18%) (near vertical P-axis; Figure 4). At 7-13 km depth about 50% of the events had normal or strike-slip faulting or mixed normal/strike-slip (P-axis oriented nearly N-S but with a variable dip and near horizontal T-axes striking E-W or NE-SW). However, 20% of the FPSs indicate more reverse faulting (S-striking T-axes dipping 20-75). Clusters 1-3 of well located events (Figure 2) mainly show normal with a mix of strike slip motion, whereas FPS of cluster 4 indicated reverse faulting (Figure S4).



The events in the main cluster (7-13 km depth) show a wide range of mechanisms. We therefore compared focal mechanisms from before the 1999 intrusion swarm (i.e., between 12 July 1996 and July 1999) to the ones in the period after the main uplift had taken place (after November 1999) to see if we would observe less scattering (Figure 4). Prior to the uplift the horizontal T-axes were predominantly oriented approximately NE-SW; the scatter is large but there is an indication of rotation to the east after the period of maximum uplift.

Following the intrusive episode in 1999/2000 two minor swarms were observed in Eyjafjallajökull volcano, in November 2004 when 13 events occurred at the location of the two main clusters, and in June and July 2006 when 11 thrust-type events occurred at 16 km depth just north of the glacier rim (cluster 4 in Figure 2 and Figure S4). GPS deformation from 2000 to 2009 suggest a significant deflation signal of the southeast flank of the volcano, consistent with cooling and contraction of the sills that formed in 1994 and 1999/2000 (Figure 5).

# 5. Discussion

*General*

The SIL-seismic catalogue from 1991 to 2009 shows that Eyjafjallajökull volcano exhibits in general very low background seismic activity, in agreement with previous studies (Einarsson and Brandsdóttir, 2000; IMO-SIL-bulletins 1955-1990, Table S9). The frequency-magnitude distribution for the complete data set yields a magnitude of completeness of $M_{lw}$=1.6 and a b-value between 1.4 and 1.6, not unusual for volcanic areas; considerably higher than typical b-values of ~0.87 found for the Hengill central volcano during a 10 year period of uplift (Ágústsson and Halldórsson, 2005) but slightly lower than b-value of 2.1 estimated for the 2007-2008 Upptyppingar intrusion event (Jakobsdóttir et al., 2008).

*Magma pathways*

The relocated earthquakes show separate clusters, but the overall pattern forms a sporadic, rather narrow, pipe-like structure, extending from the crust-mantle boundary (22-25 km) towards the surface below the mid to northern part of the ice cap. During both the 1994 and the 1999-2000 swarm, the majority of the activity was focused in the same region, forming overlapping east-west elongated, horse-shoe shaped clusters north of the center of uplift which we conclude is the location of the magma channel feeding the sill intrusions beneath the southern flank of the volcano, as suggested by Pedersen and Sigmundsson (2004 and 2006). Thus, seismicity illuminates distinct parts of the magma channel and the main cluster probably reflects the depth of maximum crustal strength, since in this depth interval (10-12 km) we also observe a peak in average stress drop (Figure 7). Earthquakes in the magma channel seem to occur both below and above our preferred depth of the modelled sills. However, we do not think it is likely that magma reached the upper cluster. These events are likely a responce to increased stress towards the surface above the channel. Uplift was not detected at the northern slopes of the volcano in connection with the filling or extraction of this magma pathway. Seismicity during 1999 indicates flow of magma from the feeder pipe southwards beneath the southern flank between August and September. The southward migration coincides with the period of maximum deformation as seen in InSAR images (Pedersen and Sigmundsson 2006; Hooper, 2009). Two out of the four small clusters in Figure 2 (1 and 2) have depths close to the intruded sill depth, with FPS indicating normal faulting (near horizontal, E-W tension axes) but cluster three is beneath the suggested depth of the sill intrusion (showing a more mix of normal and strike-slip faulting). We do not observe

441 southward migration of seismicity during the formation of the 1994 intrusion. The subtle
442 background activity we observe is largely located along the magma channel (the main cluster)
443 and above the newly formed intrusions, in the uppermost kilometers of the crust.
444
445 Two out of the three main seismic swarms observed during the observation period are located
446 in the upper crust and occur during the two periods that stand out in the GPS-time series as
447 inflation periods, in 1994 and 1999-2000, consistent with intrusions forming beneath the
448 southern flank of the volcano. Our simple horizontal, disk-shaped sill models have
449 comparable volumes to previous variable-opening-sill-models of Pedersen and Sigmundsson
450 (2004, 2006). These volume estimates, as well as the different seismic moment release for
451 these two episodes (showing ~ five times higher accumulative moment for 1999-2000) clearly
452 indicate that the 1999-2000 intrusion was larger than the one formed in 1994.
453
454 There is a large variation in focal mechanisms for the seismic events in our data set. Most of
455 these events are small, below $M_l$=2.5, which does account for some variety and furthermore
456 we did not reevaluate the picks and polarities and used the routine picks. The addition of three
457 new stations N, NE, and SE of the volcano between the two intrusion events (Figure 1a)
458 explains the slightly less scattered mechanisms for the latter intrusion swarm compared to the
459 first one. The mechanisms for the largest cluster at 7-13 km depth, before and after the
460 maximum uplift, imply a mix of a normal and strike-slip motion. The indication of eastward
461 rotation of the T-axes after the maximum uplift had taken place in 1999 probably reflects the
462 change of the local stress field due to the intruded magma, SSE of the feeding channel. For
463 the few events in the 5-7 km interval, the horizontal T-axis is oriented E-W with a dipping P-
464 axis, which infers predominantly dilatation, in contrast to the results of Dahm og Brandsdóttir
465 (1997), which suggested a thrust-type double couple mechanisms accompanied by a source
466 component for several selected events from the 1994 intrusion swarm.
467
468 *The deep activity*
469 No significant crustal deformation was detected in connection with the 1996 seismic swarm.
470 This could be due the great depth at which the activity took place, just above the crust-mantle
471 boundary, and sparse measurements at that time, with no continuously operating GPS-stations
472 near the volcano and limited ability of InSAR to resolve deformation due to deep sources
473 (Pedersen and Sigmundsson, 2006; Hooper et al., 2009). We cannot determine whether the N-
474 S elongation of the deep cluster is real and/or due to the lack of seismic stations north or south

of the cluster, which would better constrain its horizontal shape and location. Focal mechanisms for the deep swarm show predominantly near horizontal, E-W oriented tension axis (T) (Figure 4) but more variable dipping and striking pressure axis. The orientation of the T-axis suggests that extension is a dominant factor close to the crust-mantle boundary during this swarm. We conclude that the swarm indicates a short period of magma intruding from the mantle up into the bottom of the crust. The higher strain rate caused by such an intrusion results in brittle behaviour of the otherwise ductile, hot rock (Sibson, 1984). The b-value for the 13-17 km events is 1.1-1.2, but increases to a much higher b-value of 2.5-3.1 for the deepest events (17-26 km). The low accumulated seismic moment for the deep swarm and the high b-value probably reflects the higher temperature at the bottom of the crust, since it is based on the lack of large events in the ductile part of the crust.

Deep intrusion events are not commonly observed in Iceland. Rather deep events (probably ~15 km deep) were recorded beneath the Heimaey fissure in Vestmannaeyjar, just before it erupted in 1973 and in the SIL-catalogue (1991-2015) events down to 15-18 km depth have been observed.. Deep seismicity was also observed during the large swarm at Upptyppingar-Álftadalsdyngja in the northern volcanic zone in 2007-2008, when thousands of earthquakes were detected between 14-22 km depth accompanying horizontal displacement of continuous GPS stations (Jakobsdóttir et al., 2008; Hooper et al., 2011; White et al., 2011). Furthermore, in December 2007, ten small earthquakes were recorded deep below the southern coast of Iceland, near to cape Hjörleifshöfði (location is marked by an H in Figure 1). After relocation of the events using the P23-model and reevaluation of their FPS, they formed a dense cluster of normal faulting events (horizontal tension axes) located between 24 and 25 km depth (Figure S6), near the bottom of the crust. It is possible that the 1996 swarm marks the beginning of magma transport up into the crust, which later fed the 1999 intrusion.

*The contraction signal following the intrusions*

GPS measurements from 1992 show no significant inflation during seismically quiet periods (Figure S5). This is different to the behavior of some other active and well-studied volcanoes in Iceland such as Hekla volcano (seismically quiet but inflating; Ófeigsson et al., 2011; Geirsson et al., 2012) and Grímsvötn (low seismicity, inflation; Vogfjord, 2010; Hreinsdóttir et al, 2014; Reverso et al., 2014). In fact subsidence is observed following both the 1994 and 1999 inflation. Subsidence was also observed at Krafla, N-Iceland between 1992 and 1995, after a 10-year-long rifting episode (Sigmundsson et al., 1997) interpreted as contraction of

509 the magma chamber due to cooling. Assuming a contracting sill following the 1999-2000
510 intrusion we get a best fitting model at a comparable depth to the modeled intrusions, 5.5 ±
511 2.0 km, with a volume decrease of 0.0015 $km^3$/yr. This is about 5% of the intruded volume for
512 the 1999-2000 intrusion every year or 4%/yr of the combined 1994 and 1999-2000 sills'
513 volume. Following Sigmundsson et al. (1997) we estimated the volume change that could be
514 expected due to the solidification and thermal contraction of the intruded magma. We assume
515 that the magma is primitive basalt, originating at the base of the crust. The density of molten
516 gabbro is about 2700-2800 kg/$m^3$ (Olgeir Sigmarsson, personal communication 2014). We
517 assume that the density of solidified basalt at 900-950°C is around 3000 kg/$m^3$. This suggests
518 a 9% total volume decrease. We also make account for the contraction due to cooling of the
519 magma body from 950°C down to ~450°C at 5 km depth (assuming that the thermal gradient
520 at Eyjafjallajökull is 90°C/km, Sæmundsson, 1998; ISOR-database) and estimate a further
521 contraction of about 2%, or a total of about 11% expected volume reduction due to cooling
522 and contraction. The accumulated volume decrease from 2000.5 to 2009.3 is ~0.013 $km^3$ or
523 around three times larger than what one would expect due to solidification and thermal
524 contraction of the 1994 and 1999-2000 intrusions. The observed volume change can thus not
525 be explained by cooling and contraction of the sill intrusions alone. Sigmundsson et al.
526 (1997) found that the deformation rate at Krafla slowed down with time. The time series at the
527 CGPS station THEY, at the south flank of Eyjafjallajökull, do not however, appear to show
528 significant slowing down during the 2000.5-2009.3 time period (Figure 3). Long-term
529 subsidence has been observed both at Askja and Torfajökull volcanoes (Sturkell et al., 2006,
530 Scheiber et al, 2011; Geirsson et al., 2012). Measurements at Askja volcano indicate a rapid
531 deflation since at least 1983 at a slowly decaying rate due to volume change in a shallow
532 magma chamber (Sturkell and Sigmundsson, 2000, Sturkell et al., 2006, de Zeeuw-van
533 Dalfsen et al., 2013).
534
535 At volcanoes located in the divergent plate boundary zone of Iceland, rifting or stretching of
536 the plates above a weaker crust may result in subsidence. Eyjafjallajökull volcano is however
537 located in a volcanic flank zone where spreading is negligible. Studies of $CO_2$ emission at
538 Eyjafjallajökull at the Gígjökull outlet glacier (flowing northwards from the summit crater)
539 have shown that between 1993 and 2000 the volcano emitted variable but significant amounts
540 of $CO_2$ gas, or between 0.3 and 3 tons/hour (Gíslason et al., 1995; Gíslason, 2000). The $CO_2$
541 gas is released from magma during crystallization but does not necessarily escape all the way
542 up to the surface and could be discharged more slowly. We suggest that the discharge of $CO_2$

and other magmatic gases could count for some of the volume decrease observed. In addition it is possible that the intrusions cause loading of mass within the crust that results in long term adjustment of the region or that retreating and/or cooling of magma in the magma pathway plays a significant role in the unusually large volume decrease observed post the 1999-2000 intrusion.

## 6. Conclusions

Eyjafjallajökull volcano shows very subtle background activity with major swarms (of more than 100 events) occuring in connection with magmatic activity, both during upper crustal intrusive activity and deeper crust-mantle boundary events.

The overall pipe-like pattern of the earthquake distribution, extending throughout the crust below the Eyjafjallajökull volcano, indicates a channel from the crust-mantle boundary through the crust, feeding the two intrusions that were formed in the upper crust during the observation period.



The geodetic data for the 1994 and 1999-2000 intrusions can be modelled as horizontal, circular sills at ~ 5 km depth beneath the southeastern flank. The volume of the 1994 intrusion (0.011 $km^3$) was nearly three times smaller than the volume of the 1999-2000 intrusion (0.030 ± 0.007 $km^3$) and the seismic moment release approximately five times smaller.

The near horizontal, E-W oriented T-axes for the deep 1996 swarm indicate tension/opening near the base of the crust during that time, suggesting inflow of magma from below into the base of the crust.

There is no indication of shallow magma accumulation beneath Eyjafjallajökull between 1991 and 2009, the only inflation observed in geodetic data occurs during the formation of the 1994 and 1999-2000 intrusions beneath the south-eastern flank with associated seismicity.

Contraction is observed in the years following the two intrusion events. The yearly estimation of volume decrease for the latter contraction period (from July 2000 through April 2009) is -0.0015 ± 0.0003 $km^3$, with the accumulated volume decrease being three times larger than what one would expect due to solidification and thermal contraction alone. Discharge of $CO_2$

and other volcanic gases from the intrusions in addition to mass loading effects within the crust could account for this unusually large volume decrease.

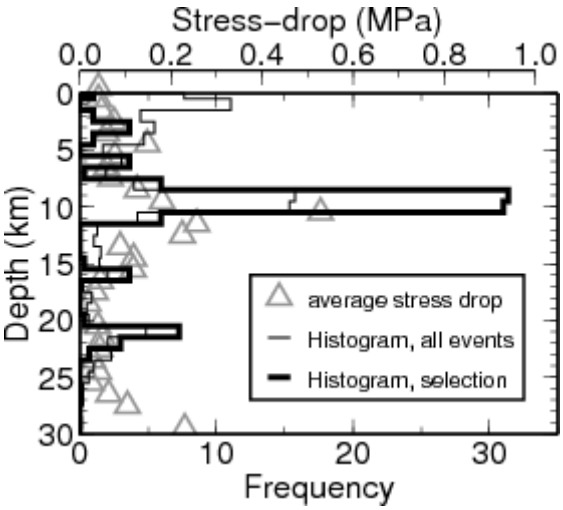


**Figure 7.** Depth-frequency plot for all relocated events (thin black line) and selected events with low relative error, within 100 m in latitude and longitude and 300 m in depth (thick line). Average stress drop for 1 km depth intervals is shown as grey triangles.
(Figure width: one column)



## Acknowledgements

This work is supported by the European Commission, 6th Framework Project 'VOLUME', Contract No. 018471, the Icelandic Research Fund (RANNÍS) project 'Volcano Anatomy' and by the European Commission-FP7 Environment Program 'FUTUREVOLC'. All figures in this paper were made with the Generic Mapping Tool public domain software (Wessel and Smith, 1998). The CGPS measurements at the site HAMR from 2006 to 2008 were collaborative effort between Rick Bennett at the University of Arizona, the Icelandic Meteorological Office, and the University of Iceland with support from RANNÍS. Many thanks to Peter Scmidt for evaluating GIA-model values for the GPS-sites and to Peter and Björn Lund for fruitful discussion about GIA and GIA-corrections. Also thanks to Freysteinn Sigmundsson (IES) for review and constructive comments on our manuscript, to Matthew J. Roberts (IMO) for review and comments on an early version of the manuscript, to Árni Hjartarson at the Iceland Geosurvey (ISOR) for providing thermal gradient data, to Bergþóra Þorbjarnardóttir (IMO) for providing pre SIL catalogue events and to Þóra Árnadóttir and Rikke Pedersen (IES) for providing model corrections for the SISZ 2000 earthquakes and discussions.

# References


Aki, K., Maximum likelihood estimate of b in the formula log N = a- b M and its confidence limits, *Bull. Earthquake Res. Inst. Univ. Tokyo*, **43**, 237-239, 1965.

Altamimi Z, L. Métivier, and X. Collilieux, 2012: ITRF2008 plate motion model, *J. Geophys. Res.*, **117** (B07402) doi:10.1029/2011JB008930.

Ágústsson, K., and P. Halldórsson, 2005. Seismic hazard in the Hengill area based on the SIL earthquake catalogue - First results. *Icelandic Meteorological Office*, report 05015.

Árnadóttir T., B. Lund, W. Jiang, H. Geirsson, H. Björnsson, P. Einarsson, and T. Sigurdsson, 2009. Glacial rebound and plate spreading: results from the first countrywide observations in Iceland. *Geophys. J. Int.*, **177**, 691-716. doi: 10.1111/j.1365-24X.2008.04059.x.

Battaglia, Maurizio, Cervelli, P.F., and Murray, J.R., 2013, Modeling crustal deformation near active faults and volcanic centers—A catalog of deformation models: U.S. Geological Survey Techniques and Methods, book 13, chap. B1, 96 p., http://pubs.usgs.gov/tm/13/b1.

Bjarnason, I. Th., W. Menke, Ó. G. Flóvenz and D. Caress, 1993. Tomographic image of the Mid-Atlantic Plate Boundary in southwest Iceland. *J. Geophys. Res*., **98**, 6607-6622.

Böðvarsson, R., S. Th. Rögnvaldsson, S. S. Jakobsdóttir, R. Slunga, and R. Stefánsson ,1996. The SIL data acquisition and monitoring system. *Seism. Res. Lett. 67*, pp. 35-46.

Bödvarsson, R., S. Th. Rögnvaldsson, R. Slunga and E. Kjartansson, 1999. The SIL data acquisition system - at present an beyond year 2000, Phys. Earth Planet. Inter., 113, 89–101.

Dahm, T., B. Brandsdóttir, 1997. Moment tensors of microearthquakes from the Eyjafjallajökull volcano in South Iceland. *Geophys. J. Int***, 130**, 183-192.Einarsson, P., B. Brandsdóttir, 2000. Earthquakes in the Mýrdalsjökull area, 1978-1985. *Jökull*, **49**, 59-73

de Zeeuw-van Dalfsen, E., H. Rymer, E. Sturkell, R. Pedersen, A. Hooper, F. Sigmundsson, B. Ófeigsson, 2013. Geodetic data shed light on ongoing caldera subsidence at Askja, Iceland. *Bull Volcanol*, **75:709**, doi: 10.1007/s00445-013-0709-2.

Einarsson, P., B. Brandsdóttir, 2000. Earthquakes in the Mýrdalsjökull area, 1978-1985. *Jökull*, **49**, 59-73

Fialko, Y., Y. Khazan, and M. Simons, 2001. Deformation due to a pressurized horizontal circular crack in an elastic half-space, with applications to volcano geodesy. *Geophys. J. Int.*, **146** (1), p. 181-190.

Geirsson, H., LaFemina, P., Árnadóttir, Th., Sturkell, E., Sigmundsson, F., Travis, M., Schmidt, P., Lund, B., Hreinsdóttir, S., Bennet, R, 2012. Volcano deformation at active plate boundaries: Deep magma accumulation at Hekla volcano and plate boundary deformation in south Iceland, *J. Geophys. Res.,* **117**, doi: 10.1029/2012JB009400

Gíslason, S. R., A. Andrésdóttir, J. H. Steingrímsson, R. F. Jósavinsson, S. Ásbjörnsson, Þ. Rúnarsson, A. Stefánsson, G. Arnardóttir, I. Karlsdóttir og Þ. Friðriksson, 1995. Koltvísýringur frá Eyjafjallajökli (Carbon dioxide from Eyjafjallajökull, in Icelandic). In: *Eyjar í eldhafi*, Pub.. Gott mál, Reykjavík, pp. 229-234.

Gíslason, S., 2000. Koltvíoxíð frá Eyjafjallajökli og efnasamsetning linda og straumvatna í nágrenni Eyjafjallajökuls og Mýrdalsjökuls ($CO_2$ from Eyjafjallaökull and the chemistry of water near Eyjafjallajökull and Mýrdalsjökull, in Icelandic). *Science Institute, University of Iceland*, report RH-06-2000.

Gutenberg, B. and C. F. Richter, 1944. Frequency of earthquakes in California. *Bulletin of the Seismological Society of America*, **34** (4). pp. 185-188. ISSN 0037-1106.

Herring, T. A, 2003. MATLAB Tools for viewing GPS velocities and time series. *GPS Solutions*, **7**, pp.194-199..

Hjaltadóttir, S., K. S. Vogfjörð, R. Slunga, 2009. Seismic signs of magma pathways through the crust in the Eyjafjallajökull volcano. *Icelandic Meteorological Office*, report, 2009-013.

Hooper, A., R. Pedersen, F. Sigmundsson, 2009. Constraints on magma intrusion at Eyjafjallajökull and Katla volcanoes in Iceland, from time series SAR Interferometry. In: *The VOLUME Project. VOLcanoes: Understanding subsurface mass moveMEnt*, edited by C. J. Bean, A. K. Braiden, I. Lokmer, F. Martini, G. S. O'Brien, p. 13-24.

Hooper, A., B. Ófeigsson, F. Sigmundsson, B. Lund, P. Einarsson, H. Geirsson, and E. Sturkell, 2011. Increased capture of magma in the crust promoted by ice-cap retreat in Iceland. *Nature Geoscience* **4**(11), 783-786, doi:10.1038/NGEO1269.

Hreinsdottir, S., F. Sigmundsson, M. J. Roberts et al. , 2014. Volcanic plume height correlated with magma-pressure change in Grímsvötn volcano, Iceland. *Nat. Geosci*., **7**, 2014-2018, doi: 10.1038/ngeo2044.

Jakobsdóttir, S. S., 1998. Uppsetning SIL-kerfisins (Installation of the SIL-network, in Icelandic). Icelandic Meteorological Office report, VÍ-G98012-JA01.

668 Jakobsdóttir, S. S., M. J. Roberts, G. B. Guðmundsson, H. Geirsson, and R. Slunga, 2008.
669 Earthquake swarms at Upptyppingar, north-east Iceland: A sign of magma intrusion?
670 *Stud. Geophys. Geod*., **52**, 513-528.
671 Jakobsdóttir, S. S., 2008. Seismicity in Iceland 1994-2007. *Jökull,* **58**, 75-100.
672 Jónsdóttir, K., A. Tryggvason, R. Roberts, B. Lund, H. Soosalu, R. Böðvarsson, 2007. Habits
673 of a glacier-covered volcano: Seismicity patterns and velocity structure of Katla
674 volcano, Iceland. Annals of Glaciology, **45**, 169-177.
675 Jónsson, B., 1774. Annalar Þess froma og velvitra Sauluga Biørns Jonssonar á Skardsau
676 Fordum Løgrettumanns í Hegranes-Sýslu (Skarðsárannáll, page 186) In Icelandic.
677 Available at http://baekur.is/bok/000043701/Annalar_THess_froma_og.
678 Jónsson, J., 1985. Þáttur um jarðfræði Eyjafjalla. Notes on the Geology of the Eyjafjöll,
679 southern Iceland (In Icelandic, summary in English). *Náttúrufræðingurinn*, **55(1)**,1-8.
680 Jónsson, J., 1988. Geological Map Eyjafjöll. Research Institute Neðri Ás, Hveragerði.
681 Larsen, G., A. J. Dugmore, and A. J. Newton, 1999. Geochemistry of historical-age silicic
682 tephras in Iceland. *Holocene 9*, 463-471.
683 Larsen, G., 2000. Holocene eruptions within the Katla volcanic system, south Iceland:
684 Characteristics and environmental impact. *Jökull*, **49**, 1-28.
685 Ófeigsson B. G., A. Hooper, F. Sigmundsson, E. Sturkell, R. Grapenthin 2011. Deep magma
686 storage at Hekla volcano, Iceland, revealed by InSAR time series analysis. J Geophys
687 Res, **116**:B05401, doi:10.1029/2010JB007576.
688 Óskarsson, B. V., 2009. *The Skerin ridge on Eyjafjallajökull, south Iceland: Morphology and*
689 *magma-ice interaction in an ice-confined silicic fissure eruption*, Master's thesis,
690 Faculty of Earth Sciences, University of Iceland, pp. 111. Available at:
691 http://hdl.handle.net/1946/4375.
692 Pedersen, R., S. Jónsson, T. Árnadóttir, F. Sigmundsson, K.L. Feigl, 2003. Fault slip
693 distribution of two June 2000 $M_W$ 6.5 earthquakes in South Iceland estimated from joint
694 inversion of InSAR and GPS measurements. *Earth and Planetary Science Letters,* **213**
695 (3), 487-502.
696 Pedersen, R., F. Sigmundsson, 2004. InSAR based sill model links spatially offset areas of
697 deformation and seismicity for the 1994 unrest episode at Eyjafjallajökull volcano,
698 Iceland. *Geophys. Res. Lett*. **31**: L14610, doi:10.1029/2004GL020368.
699 Pedersen, R., F. Sigmundsson, 2006. Temporal development of the 1999 intrusive episode in
700 the Eyjafjallajökull volcano, Iceland, derived from InSAR images. *Bull. Volcanol*. **68**:
701 377-393. Doi:10.1007/s00445-005-0020-y.

Reverso, T., J. Vandemeulebrouck, F. Jouanne, V. Pinel. T. Villemin, E. Sturkell, and P. Bascou, 2014. A two-magma chamber model as a source of deformation at Grímsvötn Volcano, Iceland, J. Geophys. Res. Solid Earth, **119**, 46666-4683, doi:10.1002/2013JB010569.

Rögnvaldsson, S. Th. and R. Slunga, 1993. Routine fault plane solutions for local networks: a test with synthetic data. *Bull. Seism. Soc. Am*., **83**, 4, 1232-1247.

Rögnvaldsson, S. Th. and R. Slunga, 1994. Single and joint fault plane solutions for microearthquakes in South Iceland. *Tectonophysics,* 237, 73-86.

Scheiber-Enslin, S. E., P. LaFemina, E. Sturkell, A. J. Hooper, S. J. Webb, 2011. Investigation of plate spreading along a propagating ridge: The Eastern Volcanic Zone, Iceland. *Geophys. J. Int*., **187**, 1175-1194, doi:10.1111/j.1365-246X.2011.05243.x

Schmidt, P., B. Lund, C. Hieronymus, J. Maclennan, T. Árnadóttir, and C. Pagli, 2013. Effects of present-day deglaciation in Iceland on mantle melt production rates. *J. Geophys. Res.: Solid Earth* **118** (7), 3366-3379.

Sibson, R. H., 1984. Roughness at the Base of the Seismogenic Zone: Contributing Factors.*J. Geophys. Res*., **89**, B7, 5791-5799.

Sigmundsson, F., H. Vadon, and D. Massonnet, 1997. Readjustment of the Krafla spreading segment to crustal rifting measured by Satellite Radar Interferometry. *Geophys. Res. Lett*., **24** (15), 1843-1846.

Sigmundsson, F., S. Hreinsdóttir, A. Hooper, Th. Árnadóttir, R. Pedersen, M. J. Roberts, N. Óskarsson, A. Auriac, J. Decriem, P. Einarsson, H. Geirsson, M. Hensch, B. G. Ófeigsson, E. Sturkell, H. Sveinbjörnsson, and K. Feigl, 2010. Intrusion triggering of the 2010 Eyjafjallajökull explosive eruption, *Nature,* 468, pp. 426-430.

Skjálftabréf (Seismological letter, in Icelandic) nr 38, Sept. 1979. *Science Institute, University of Iceland and Icelandic Meteorological Office,* report.

Slunga, R., S. T. Rögnvaldsson and R. Bödvarsson, 1995. Absolute and relative locations of similar events with application to microearthquakes in southern Iceland. *Geophys. J. Int*., **123**, 409-419.

Soosalu, H., K. Jónsdóttir, P. Einarsson, 2006. Seismicity crisis at the Katla volcano, Iceland – signs of a cryptodome? J. Volcanol. Geotherm. Res. 153, 177-186.

Stefánsson R., R. Böðvarsson, R. Slunga, P. Einarsson, S. Jakobsdóttir, H. Bungum, S. Gregersen, J. Havskov, J. Hjelme, H. Korhonen, 1993. Earthquake prediction research

in the south Iceland seismic zone and the SIL project. *Bull. Seism. Soc. Am.*, 83, no. 3, 696-716.

Sturkell E., F. Sigmundsson, 2000. Continuous deflation of the Askja caldera Iceland, during the 1983-1998 non-eruptive period, *J Geophys Res*, 105:25671- 25684.

Sturkell, E., F. Sigmundsson, and P. Einarsson, 2003. Recent unrest and magma movements at Eyjafjallajökull and Katla volcanoes, Iceland. *J. Geophys. Res*. **108**:2, doi: 2310.1029/2001JB000917.

Sturkell E, P. Einarsson, F. Sigmundsson, H. Geirsson, H. Ólafsson, R. Pedersen, E. Zeeuw-van Dalfsen, A. L. Linde, I. S. Sacks, and R. Stefánsson, 2006. Volcano geodesy and magma dynamics in Iceland, *J Volcanol Geotherm Res*, 150:14-34.

Sturkell, E., P. Einarsson, F. Sigmundsson, A. Hooper, A., B. G. Ófeigsson, H. Geirsson, H. Ólafsson, 2010. Katla and Eyjafjallajökull Volcanoes, *Dev. Quater. Sci.,* **13**.

Sæmundsson, K., 1979. Outline of the geology of Iceland. *Jökull* **29**, 7-28.

Sæmundsson, K., 1998. Heitavatnsborun í Sólheimahjáleigu í Mýrdal, *National Energy Authority report (Orkustofnun Greinargerð)* KS-98-09.

Sæmundsson, K., and P. Einarsson, 1987. Geological map of Iceland, sheet 3, SW-Iceland, second ed. – *Museum of Natural History and the Iceland Geodetic Survey*, Reykjavík.

Tarasewicz, J., R. S. White, B. Brandsdóttir and B. S. Thorbjarnardóttir, 2011. Location accuracy of earthquake hypocentres beneath Eyjafjallajökull, Iceland, prior to the 2010 eruptions. *Jökull* **61**, 33-50.

Thoroddsen, Th., 1925). *Die Gesichte der Islandischen Vulkane – nach einem hinterlassenen Manuscript,* D. Kgl. Danske Vidensk. Selsk. Skrifter, Nat. og Mathem. Afd. 8, Række IX, Köbenhavn, pp. 458.

Vogfjörd, K. S., G. Nolet, W. J. Morgan, R. M. Allen, R. Slunga, B. H. Bergsson, P. Erlendsson, G. Foulger, S. Jakobsdóttir, B. Julian, M. Pritchard, S. Ragnarsson, 2002. Crustal profiling in Iceland using earthquakes source arrays, AGU Fall meeting, Abstract S61C-1161, San Francisco, California, 6-10 December, 2002.

Vogfjord, K. S., 2010. Seismicity and tremor signals associated with magma movements in Icelandic volcanoes, Abstract V21F-07 presented at 2010 Fall Meeting, AGU, San Francisco, Calif., 13-17 Dec.

Waldhauser, F., and W. L. Ellsworth, 2000. A double-difference earthquake algorithm: Method and application to the northern Hayward Fault, California. *Bull. Seismol. Soc. Am.,* **90**, 1353-1368.

Wessel, P. and W. H. F. Smith, 1998. New, improved version of Generic Mapping Tools released. *EOS, Trans. AGU* **79**, 579.

White, R. S., J. Drew, H. R. Martens, J. Key, H. Soosalu, S. S. Jakobsdóttir, 2011. Dynamics of dyke intrusion in the mid-crust of Iceland. Earth Planet. Sci. Lett., **304**, 300–312.

Wiemer, S.. A software package to analyse seismicity: ZMAP. Seismol. Res. Lett., 72, 3, 373-382, 2001

Wyss, M., K. Shimazak, and S. Wiemer, 1997. Mapping active magma chambers by b-values beneath the off-Ito volcano, Japan. *J. Geophys. Res*, **102**, 20413-20422.

# Online supplement

| *SITE* | *NAME* | *NUM* | *YEAR* | *LAT* | *LON* | *H (m)* |
|---|---|---|---|---|---|---|
| VMEY | Vestmannaeyjar (CGPS) | NE0002 | 2000 | 63.426989 | -20.293560 | 135 |
| HEEY | Heimaey I | LM0353 | 1992 | 63.418372 | -20.289345 | 132 |
| SEJA | Seljaland | LM0354 | 1992 | 63.611158 | -19.991277 | 140 |
| HAMR | Hamragardar | OS7487 | 1989 | 63.622447 | -19.985675 | 160 |
| MORK | Midmork | NE9909 | 1999 | 63.656980 | -19.894543 | 172 |
| HVAM | Hvammur | VRH7601 | 1999 | 63.572802 | -19.877412 | 73 |
| DAGM | Dagmalafjall | NE9420 | 1994 | 63.628382 | -19.834854 | 750 |
| MOLN | Moldnupur | NE9908 | 1999 | 63.567554 | -19.792628 | 112 |
| THEY | Thorvaldseyri (CGPS) | NE0001 | 2000 | 63.561467 | -19.643420 | 195 |
| SELJ | Seljavellir | NE9404 | 1994 | 63.562472 | -19.632632 | 265 |
| STEI | Steinsholt | NE9405 | 1994 | 63.677061 | -19.608515 | 289 |
| EINH | Einhyrningur NA | OS7385 | 1986 | 63.753687 | -19.450484 | 624 |
| SKOG | Skoga | OS7486 | 1989 | 63.576449 | -19.445499 | 670 |
| FIMM | Fimmvorduhals | NE9203 | 1992 | 63.606686 | -19.437680 | 921 |
| GOLA | Godaland (CGPS) | NE200302 | 2003 | 63.659700 | -19.322084 | 1260 |
| SOLH | Solheimar | NE9215 | 1992 | 63.507094 | -19.305339 | 272 |
| SOHH | Solheimaheidi | NE9214 | 1992 | 63.548348 | -19.258151 | 787 |
| SOHO | Solheimaheidi (CGPS) | NE9905 | 1999 | 63.552474 | -19.246644 | 858 |
| REYN | Reynisfjall II | OS7377 | 1986 | 63.418461 | -19.027266 | 298 |
| REYF | Reynisfjall I | LM0352 | 1993 | 63.418897 | -19.026441 | 302 |
| STOR | Stórólfshvoll | NE200103 | 2004 | 63.752670 | -20.212085 | 125 |

**Table S1**. List of GPS sites and when they were installed.



| *SITE* | *LAT* | *LON* | *H (m)* | *92* | *93* | *94* | *95* | *98* | *99* | *00* | *01* | *02* | *03* | *04* | *05* | *06* | *07* | *08* | *09* |
|---|---|---|---|---|---|---|---|---|---|---|---|---|---|---|---|---|---|---|---|
| VMEY | 63.426989 | -20.293560 | 135 | | | | | | | C | C | C | C | C | C | C | C | C | C |
| HEEY | 63.418372 | -20.289345 | 132 | | X | | | | | | X | | | X | | | | | |
| SEJA | 63.611158 | -19.991277 | 140 | | X | | | | X | | X | | | X | | | | | |
| HAMR | 63.622447 | -19.985675 | 160 | X | X | X | X | X | X | X | X | X | X | X | X | C | C | X | X |
| MORK | 63.656980 | -19.894543 | 172 | | | | | | X | X | X | X | X | X | X | | | | |
| HVAM | 63.572802 | -19.877412 | 73 | | | | | | X | X | X | | | | X | | | | |
| DAGM | 63.628382 | -19.834854 | 750 | | | | | X | X | X | | | | | X | | | | |
| MOLN | 63.567554 | -19.792628 | 112 | | | | | | X | X | X | | | | X | | X | | |
| THEY | 63.561467 | -19.643420 | 195 | | | | | | | C | C | C | C | C | C | C | C | C | C |
| SELJ | 63.562472 | -19.632632 | 265 | | | X | | X | X | X | X | | | | | | | | |
| STEI | 63.677061 | -19.608515 | 289 | | | X | | X | X | X | X | | | | X | | | | X |
| EINH | 63.753687 | -19.450484 | 624 | | X | | X | | | X | X | | | X | X | | | | |
| SKOG | 63.576449 | -19.445499 | 670 | X | | X | | X | X | X | X | | | | X | | | | X |
| FIMM | 63.606686 | -19.437680 | 921 | X | | X | | X | X | X | X | | | | X | | | | X |
| GOLA | 63.659700 | -19.322084 | 1260 | | | | | | | | | | X | X | X | C | C | C | C |
| SOLH | 63.507094 | -19.305339 | 272 | X | X | X | | | X | X | X | | | | X | | X | | |
| SOHH | 63.548348 | -19.258151 | 787 | X | X | X | | | X | X | X | X | | X | | | | | |
| SOHO | 63.552474 | -19.246644 | 858 | | | | | | C | C | C | C | C | C | C | C | C | C | C |
| REYN | 63.418461 | -19.027266 | 298 | X | X | X | X | X | X | X | X | X | X | X | X | X | X | | |
| REYF | 63.418897 | -19.026441 | 302 | | X | | | | X | X | X | | | X | | | | | |
| STOR | 63.752670 | -20.212085 | 125 | | | | | | | | | | | C | C | C | C | C | C |

**Table S2.** List of measurements at GPS-sites. X: campaign measurement, C: continuously recording.

| *SITE* | *E (mm)* | *N (mm)* | *dE (mm)* | *dN (mm)* | *V (mm)* | *dV (mm)* |
|---|---|---|---|---|---|---|
| REYN | -4 | 3 | 7 | 5 | -12 | 16 |
| STEI | 3 | 16 | 4 | 4 | -7 | 13 |
| SELJ | -54 | -118 | 4 | 5 | 113 | 16 |
| HAMR | 3 | 1 | 3 | 3 | -15 | 10 |
| SKOG | 70 | -14 | 7 | 5 | 29 | 16 |
| FIMM | 61 | 26 | 5 | 5 | 35 | 16 |
| DAGM | -10 | 6 | 2 | 3 | 2 | 11 |

**Table S3.** Estimated offset due to the 1999-2000 intrusion with 1 sigma uncertainties.

| *SITE* | *E (mm)* | *N (mm)* | *dE (mm)* | *dN (mm)* | *V (mm)* | *dV (mm)* |
|---|---|---|---|---|---|---|
| REYN | 4 | -3 | 3 | 3 | 8 | 8 |
| STEI | -8 | -12 | 5 | 5 | -11 | 17 |
| SELJ | -20 | -19 | 5 | 6 | 29 | 21 |
| HAMR | -3 | 9 | 5 | 5 | 5 | 15 |
| SKOG | 43 | -38 | 13 | 9 | 10 | 26 |
| FIMM | 60 | -2 | 10 | 7 | 17 | 21 |

**Table S4.** Estimated offset due to the 1994 intrusion with 1 sigma uncertainties.

| *SITE* | *E (mm/yr)* | *N (mm/yr)* | *dE (mm/yr)* | *dN (mm/yr)* | *corrEN* | *V (mm/yr)* | *dV (mm/yr)* | *GIAcorr N (mm/yr)* | *GIAcorr E (mm/yr)* | *GIAcorr V (mm/yr)* |
|---|---|---|---|---|---|---|---|---|---|---|
| VMEY | -0.20 | -0.37 | 0.03* 0.07 | 0.04* 0.07 | 0.037 | 2.9 | 0.1* 0.3 | -0.7 | -0.802951418894 | 4.1992450826 |
| HAMR | -1.92 | -1.15 | 0.04* 0.20 | 0.06* 0.20 | 0.032 | 6.1 | 0.2* 0.6 | -0.8 | -1.17638703118 | 6.0515259977 |
| MORK | -1.86 | -1.77 | 0.25 | 0.36 | 0.030 | 6.2 | 1.2 | -0.8 | -1.27056352357 | 6.6076791378 |
| HVAM | -0.74 | -2.66 | 0.34 | 0.47 | 0.102 | 7.7 | 1.5 | -1.0 | -1.16556988716 | 6.2338925324 |
| DAGM | -1.76 | -3.35 | 0.47 | 0.69 | 0.030 | 6.8 | 2.3 | -0.9 | -1.29560036772 | 6.8109797873 |
| MOLN | -0.67 | -1.25 | 0.27 | 0.38 | -0.002 | 6.4 | 1.3 | -1.1 | -1.18986876705 | 6.5926195860 |
| THEY | 0.09 | 1.24 | 0.02* 0.12 | 0.02* 0.10 | 0.008 | 4.2 | 0.1* 0.3 | -1.3 | -1.15077573431 | 7.2988933487 |
| STEI | -1.52 | -3.94 | 0.42 | 0.54 | 0.008 | 10.9 | 1.7 | -0.7 | -1.3025723492 | 8.3875702343 |
| FIMM | -5.71 | -3.22 | 0.43 | 0.59 | 0.050 | 10.7 | 1.9 | -1.3 | -1.17515239041 | 8.9785071454 |
| SKOG | -3.84 | -0.59 | 0.41 | 0.54 | 0.057 | 5.1 | 1.7 | -1.4 | -1.11037678895 | 8.4038214167 |
| SOLH | -1.15 | -4.15 | 0.31 | 0.41 | 0.008 | 9.6 | 1.4 | -1.6 | -0.811895964208 | 7.9079439534 |
| SOHO | -1.83 | -4.63 | 0.02* 0.14 | 0.03* 0.11 | 0.033 | 10.7 | 0.1* 0.4 | -1.8 | -0.890724293875 | 9.1242725234 |
| REYN | 0.15 | -2.42 | 0.18 | 0.24 | 0.017 | 7.2 | 0.7 | -1.6 | -0.352492364404 | 6.9673763092 |
| STOR | -2.62 | -0.64 | 0.04* 0.3 | 0.05* 0.3 | 0.017 | 6.4 | 0.2* 0.6 | -0.7 | -1.15431322318 | 5.7357190035 |
| SEJA | -1.75 | -2.03 | 0.63 | 0.94 | 0.017 | 6.5 | 3.1 | -0.8 | -1.16173741594 | 5.9712512733 |
| ALFT | -1.78 | -3.46 | 0.37 | 0.49 | 0.031 | 6.9 | 1.6 | -1.7 | -0.614659827965 | 7.8780705474 |
| SOHH | -2.51 | -4.95 | 0.56 | 0.74 | 0.013 | 5.3 | 2.4 | -1.7 | -0.87968274557 | 8.9266778774 |
| GOLA | -1.36 | -2.73 | 0.07* 0.7 | 0.09* 0.3 | 0.042 | 13.1 | 0.3* 1.1 | -1.0 | -1.26228064038 | 10.633143026 |
| ENTA | -3.13 | -0.91 | 0.09 | 0.12 | 0.015 | 15.7 | 0.4 | -0.9 | -0.998314693966 | 11.671060431 |
| AUST | -1.94 | -3.13 | 0.08 | 0.11 | 0.016 | 14.6 | 0.4 | -1.2 | -0.670901987039 | 11.839258407 |
| EINH | -1.98 | -0.95 | 0.55 | 0.77 | 0.012 | 12.1 | 2.5 | -0.7 | -1.3330335381 | 9.0781954077 |



**Table S5.** Estimatd velocities in the ITRF08 EURA reference frame with 1 sigma (*formal) uncertainties during the period 2000.5 – 2009.3 and correction due to GIA 2001-2009 (model D3-B81_3 from Peter Schmidt, personal communication 2014, Peter Schmidt et al., 2013).

| *SITE* | *E (mm/yr)* | *N (mm/yr)* | *dE (mm/yr)* | *dN (mm/yr)* | *corrEN* | *V (mm/yr)* | *dV (mm/yr)* |
|---|---|---|---|---|---|---|---|
| HAMR | -1.7 | -0.5 | 2.0 | 1.8 | -0.099 | 4 | 5 |
| SOLH | 1.5 | -0.9 | 4.6 | 4.8 | -0.197 | 7 | 13 |
| SOHH | 1.0 | -1.2 | 4.6 | 3.4 | -0.160 | 4 | 11 |
| REYN | 0.7 | -0.5 | 1.6 | 1.3 | -0.103 | -3 | 4 |

**Table S6.** Estimated velocities in the ITRF08 EURA reference frame with 1 sigma uncertainties during the period 1992.6 – 1994.4.

| *SITE* | *E (mm/yr)* | *N (mm/yr)* | *dE (mm/yr)* | *dN (mm/yr)* | *corrEN* | *V (mm/yr)* | *dV (mm/yr)* |
|---|---|---|---|---|---|---|---|
| HAMR | -2.0 | 1.1 | 1.0 | 0.9 | -0.072 | 0 | 3 |
| SELJ | -1.0 | -0.0 | 1.2 | 1.4 | -0.061 | 5 | 5 |
| STEI | -2.2 | 2.8 | 1.3 | 1.4 | -0.057 | 8 | 5 |
| FIMM | -4.0 | -2.1 | 1.2 | 1.3 | 0.005 | 3 | 4 |
| SKOG | -2.7 | 0.7 | 1.6 | 1.3 | 0.074 | 7 | 4 |
| REYN | 2.3 | -0.9 | 1.5 | 1.1 | 0.007 | 6 | 3 |

**Table S7.** Estimated velocities in the ITRF08 – EURA reference frame with 1 sigma uncertainties during the period 1994.7 – 1998.6.

| *SITE* | *EAST (m)* | *NORTH (m)* | *UP (m)* |
|---|---|---|---|
| DAGM | 0.0104 | -0.0128 | -0.0032 |
| ENTA | 0.0056 | -0.0048 | -0.0017 |
| FIMM | 0.0071 | -0.0072 | -0.0023 |
| HAMR | 0.0095 | -0.0126 | -0.0029 |
| HVAM | 0.0075 | -0.0098 | -0.0025 |
| MOLN | 0.0075 | -0.0094 | -0.0025 |
| MORK | 0.0123 | -0.0155 | -0.0036 |
| REYN | 0.0032 | -0.0033 | -0.0012 |
| SELJ | 0.0071 | -0.0082 | -0.0024 |
| SKOG | 0.0066 | -0.0068 | -0.0022 |
| SOHH | 0.0051 | -0.0051 | -0.0017 |
| SOLH | 0.0048 | -0.0050 | -0.0017 |
| STEI | 0.0109 | -0.0110 | -0.0031 |
| THEY | 0.0071 | -0.0083 | -0.0024 |
| SEJA | 0.0095 | -0.0126 | -0.0029 |
| SOHO | 0.0051 | -0.0050 | -0.0017 |
| AUST | 0.0047 | -0.0041 | -0.0015 |



**Table S8.** Estimated offsets due to the two ~M6.5 June 2000 earthquakes in the SISZ from Pedersen et al., (2003).

| Year-d-mm | OT | Lat | Lon | Depth | Ml | Mcoda | Num. stations | Num. phases |
|---|---|---|---|---|---|---|---|---|
| 1969-10-30 | 01:41:10.0 | 63.6 | -19.5 | (null) | 3.2 | (null) | 4 | 8 |
| 1971-10-09 | 12:55:18.0 | 63.6 | -19.5 | (null) | 2.6 | (null) | 3 | 5 |
| 1972-12-20 | 01:30:08.0 | 63.6 | -19.5 | (null) | 2.9 | (null) | 3 | 5 |
| 1973-12-05 | 18:00:10.0 | 63.6 | -19.7 | (null) | 2.4 | (null) | 1 | 10 |
| 1979-06-16 | 04:47 | 63.63* | -19.56* | (null) | 2.0 | (null) | (null) | (null) |
| 1979-06-29 | 20:22 | 63.63* | -19.56* | (null) | small | (null) | (null) | (null) |
| 1979-07-03 | 05:59 | 63.63* | -19.56* | (null) | 1.5 | (null) | (null) | (null) |
| 1986-01-10 | 13:54:26.23 | 63.639 | -19.555 | 5.12 | 2.1 | (null) | 13 | 16 |
| 1987-08-13 | 05:27:19.94 | 63.605 | -19.593 | 4.98 | 2.7 | 2.6 | 14 | 16 |
| 1987-08-16 | 06:29:17.36 | 63.595 | -19.529 | 7.12 | 2.5 | 2.6 | 5 | 5 |
| 1987-09-26 | 10:38:47.33 | 63.585 | -19.529 | 5.01 | (null) | 3.0 | 4 | 4 |
| 1988-10-05 | 21:44:58.76 | 63.619 | -19.559 | 3.17 | 2.8 | 2.5 | 6 | 6 |
| 1988-10-15 | 12:56:26.28 | 63.558 | -19.535 | 4.29 | 2.8 | 2.8 | 6 | 6 |
| 1988-11-01 | 09:11:26.84 | 63.604 | -19.681 | 4.03 | 2.8 | 2.7 | 5 | 6 |

**Table S9**. Earthquakes in Eyjafjallajökull 1955-1990 from the IMO-database and Skjálftabréf, 1979. Latitudes and longitudes marked with * were estimated from Figure 2 in Einarsson and Brandsdóttir (2000).

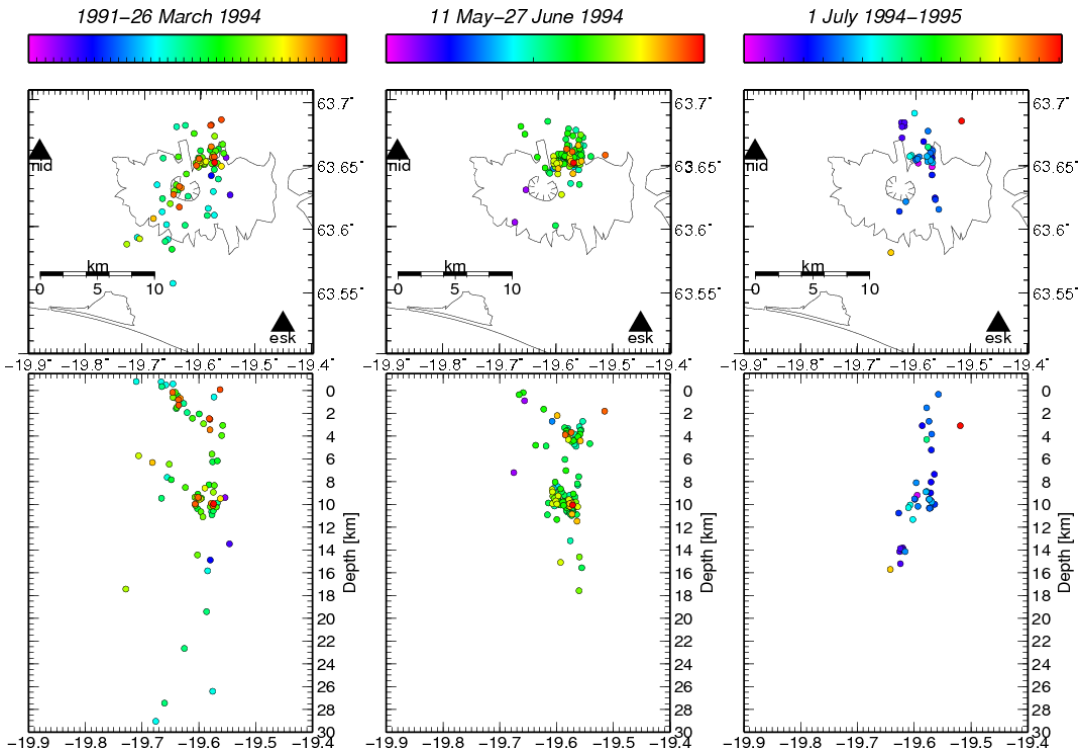


**Figure S1.** Seismicity 1991-1995 shown in map view and vertical cross section viewed from south. Events are coloured according to origin time and the bar above each map shows the time span of each map.



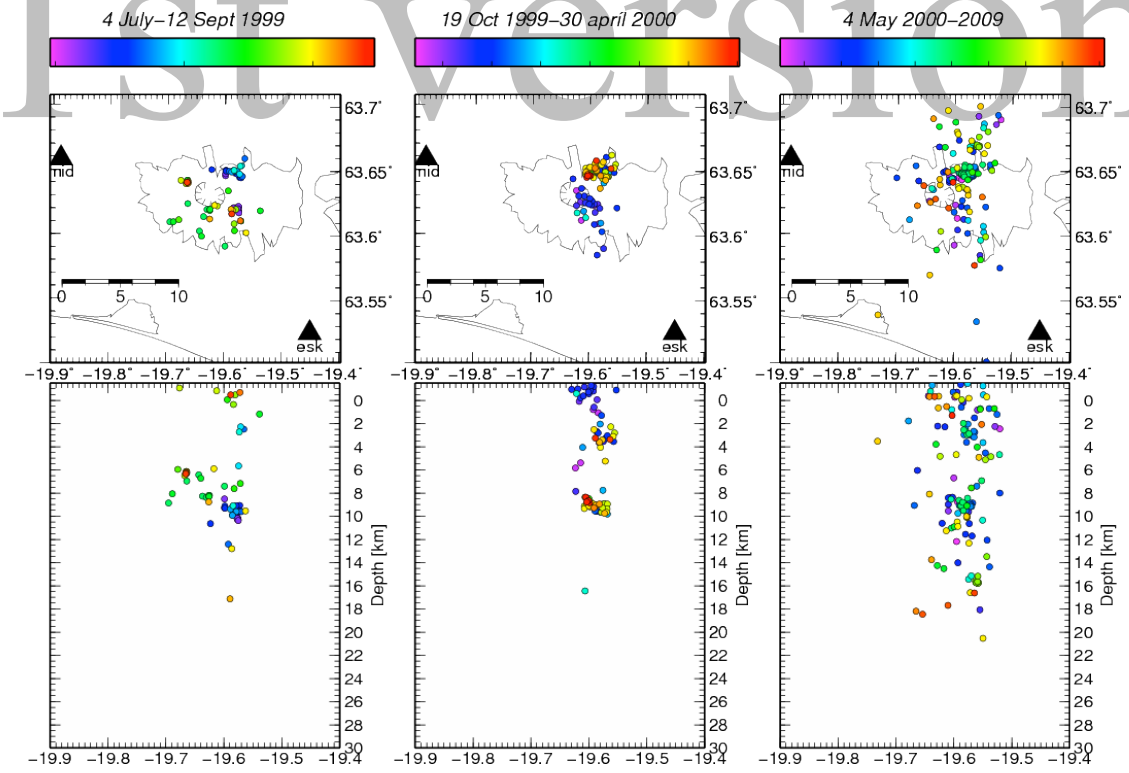


**Figure S2.** Seismicity from 1996 through April 2000.

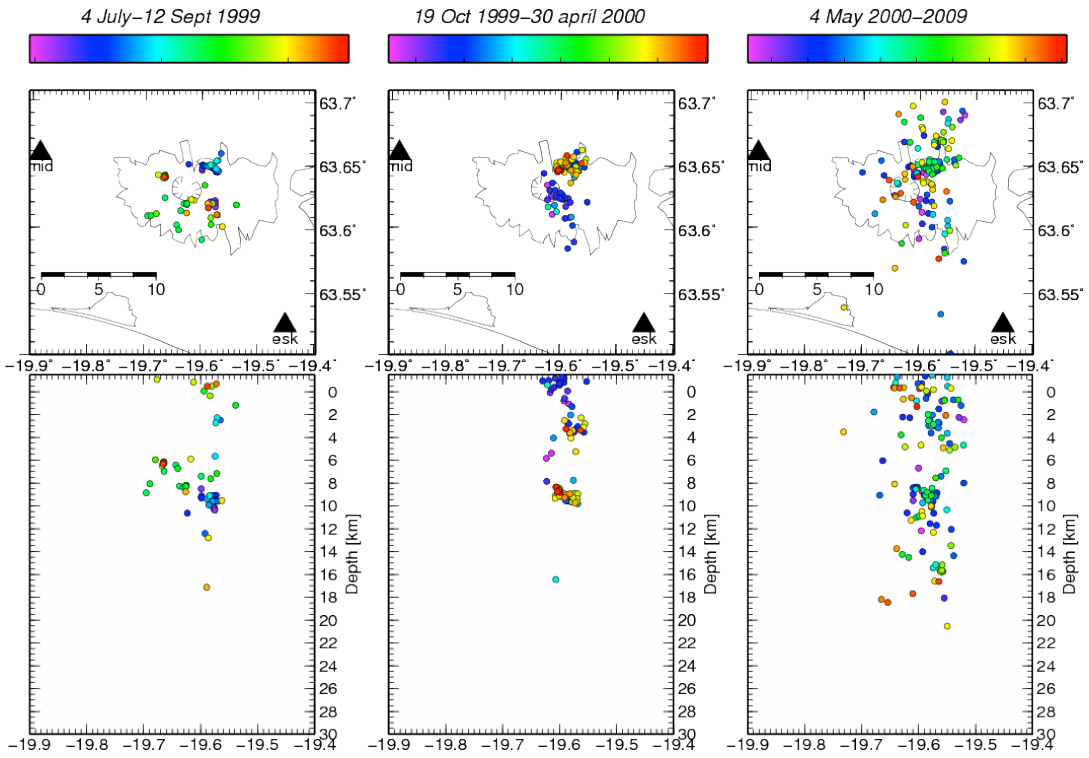


826
827
828 **Figure S3.** Seismicity from 4 July 1999 through February 2009.
829

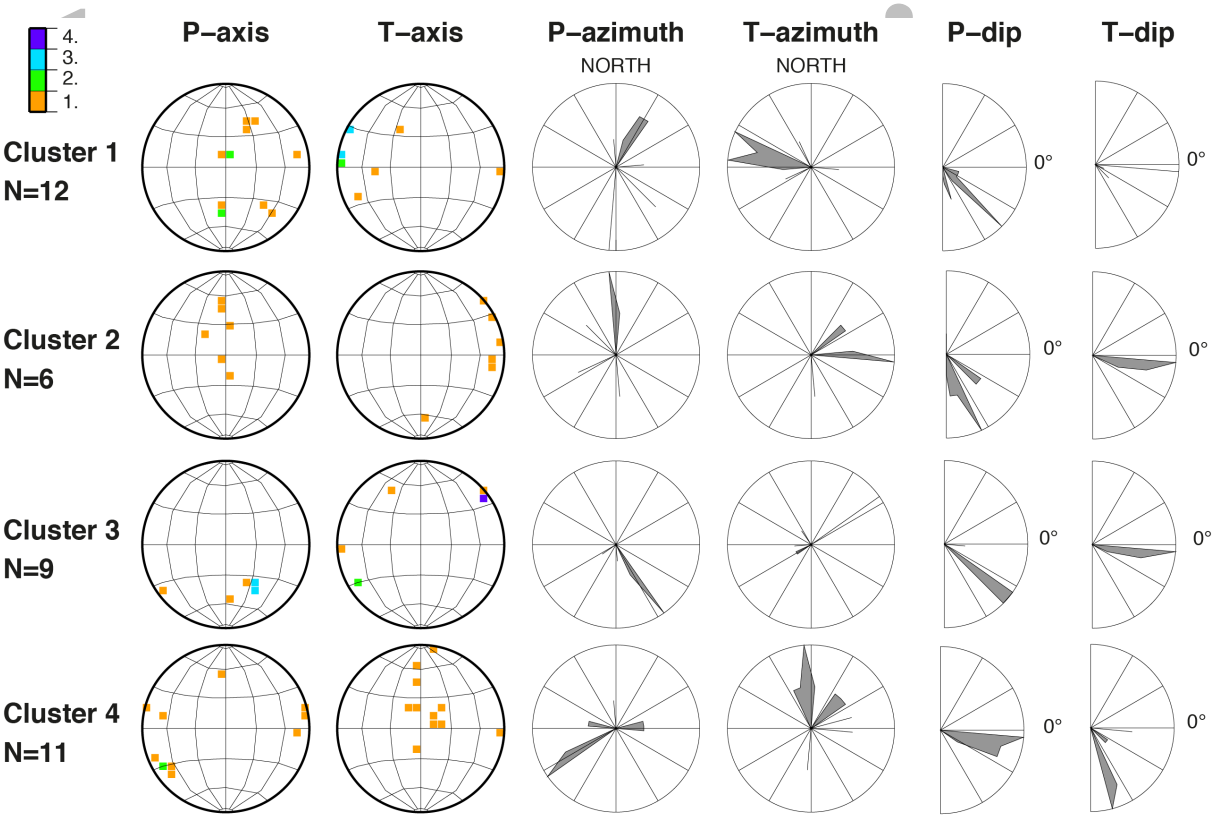


830
831 **Figure S4**. Orientation and dip of P- and T-axis for the four small clusters (numbered 1-4) in
832 Figure 2c. The number of events for each cluster is given below cluster number. The FPS for
833 the first three clusters mainly show normal faulting but for the last one (and the deepest, from
834 year 2006) mostly reverse faulting.
835 (Figure width: 1.5 columns?)

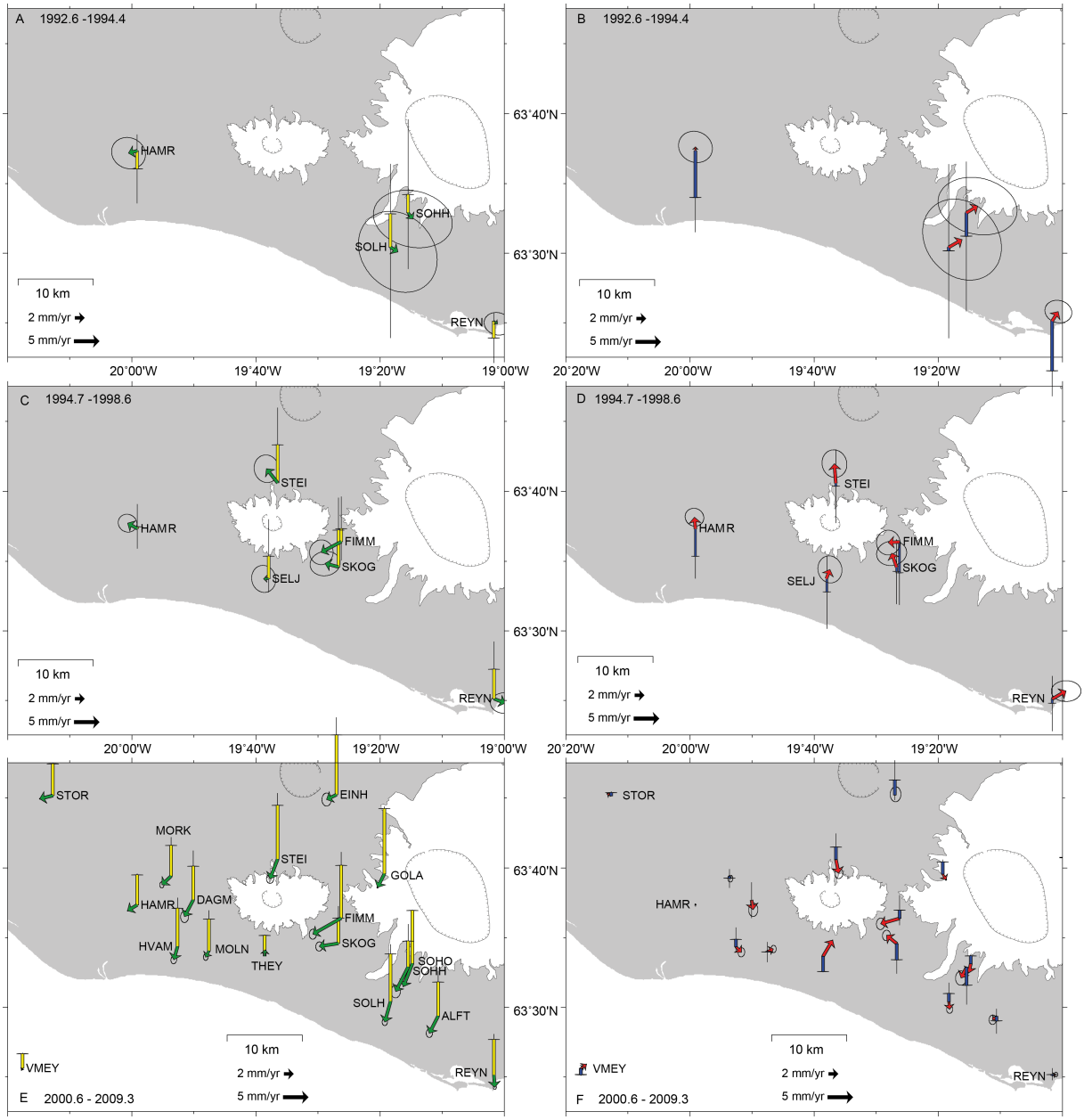


**Figure S5.** Yearly displacements for seismically quiet periods. Panels on the left (A, C, E) show data before GIA-correction (green for horizontal, yellow for vertical), panels on the right (B, D, F) show GIA-corrected data (red for horizontal, blue for vertical, with scaling of 1.6 for horizontal components).

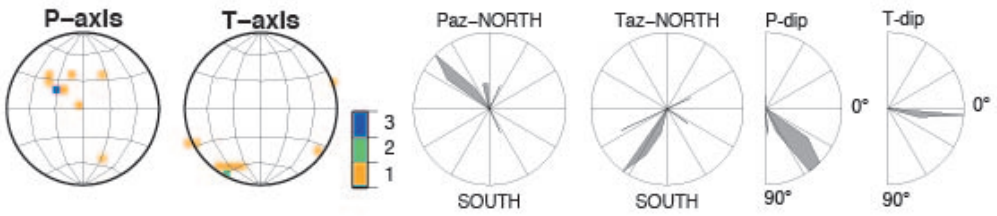


**Figure S6.** The 7-December-2007-swarm near to cape Hjörleifshöfði, ~30 km southeast of the Katla caldera, ~50 km southeast of Eyjafjallajökull volcano. The 11 events have been relocated using model P23 and form a dence cluster at 24-25 km depth. Their FPSs have

horizontal T-axis oriented mainly SW-NE to SSW-NNE and dipping P-axes, indicating predominantly normal faulting or opening. Width: two columns.